Theor Appl Genet (2011) 122:831–854
DOI 10.1007/s00122-010-1490-7

ORIGINAL PAPER

Isolation, fine mapping and expression profiling of a lesion mimic genotype, *spl*$^{NF4050-8}$ that confers blast resistance in rice

Raman Babu · Chang-Jie Jiang · Xin Xu · Kameswara Rao Kottapalli · Hiroshi Takatsuji · Akio Miyao · Hirohiko Hirochika · Shinji Kawasaki

Received: 11 February 2010 / Accepted: 4 November 2010 / Published online: 4 December 2010

Abstract We evaluated a large collection of Tos17 mutant panel lines for their reaction to three different races of *Magnaporthe oryzae* and identified a lesion mimic mutant, NF4050-8, that showed lesions similar to naturally occurring spl5 mutant and enhanced resistance to all the three blast races tested. Nested modified-AFLP using *Tos17*-specific primers and southern hybridization experiments of segregating individuals indicated that the lesion mimic phenotype in NF4050-8 is most likely due to a nucleotide change acquired during the culturing process and not due to *Tos17* insertion per se. Inheritance and genetic analyses in two japonica × indica populations identified an overlapping genomic region of 13 cM on short arm of chromosome 7 that was linked with the lesion mimic phenotype. High-resolution genetic mapping using 950 F_3 and 3,821 F_4 plants of NF4050-8 × CO39 delimited a 35 kb region flanked by NBARC1 (5.262 Mb) and RM8262 (5.297 Mb), which contained 6 ORFs; 3 of them were 'resistance gene related' with typical NBS–LRR signatures. One of them harbored a NB–ARC domain, which had been previously demonstrated to be associated with cell death in animals. Microarray analysis of NF4050-8 revealed significant up-regulation of numerous defense/pathogenesis-related genes and down-regulation of heme peroxidase genes. Real-time PCR analysis of WRKY45 and PR1b genes suggested possible constitutive activation of a defense signaling pathway downstream of salicylic acid but independent of NH1 in these mutant lines of rice.

Communicated by J.-B. Veyrieras.

R. Babu (✉) · C.-J. Jiang · X. Xu · K. R. Kottapalli · H. Takatsuji · A. Miyao · H. Hirochika · S. Kawasaki (✉)
National Institute of Agrobiosciences (NIAS), Kannon-dai 2-1-2, Tsukuba, Ibaraki 305-8602, Japan
e-mail: r.babu@cgiar.org

S. Kawasaki
e-mail: kawasa@nias.affrc.go.jp

Present Address:
R. Babu
CIMMYT, Apdo Postal 6-641, 06600 Mexico, D.F., Mexico

Introduction

Lesion mimic mutants in plants form spontaneous lesions in the absence of pathogen attack. These mutants were initially reported in maize (Hoisington et al. 1982) but later became almost ubiquitous in many other species viz., Arabidopsis (Greenberg and Ausubel 1993; Dietrich et al. 1994; Greenberg et al. 1994), rice (Takahashi et al. 1999; Yin et al. 2000; Zeng et al. 2004; Wu et al. 2008), barley (Wolter et al. 1993), wheat (Nair and Tomar 2001) and groundnut (Badigannavar et al. 2002). They have been described by various names such as lesion simulating disease (lsd) or accelerated cell death (acd) mutants in Arabidopsis, spotted leaf mutants (spl) in rice, leaf flecking mutants in wheat and disease lesion mimics or more appropriately, lesioned phenotypes in maize (Johal 2007). The phenotypes of these mutants show a broad array of variation in lesion number, size, color, pattern as well as timing and condition of lesion appearance. Depending on the behavior of lesions following inception, lesion mimic mutants are classified into either 'determinative' or 'propagative' class (Dangl et al. 1996; Johal et al. 1995; Lorrain et al. 2003; Johal 2007). In determinative mimics, lesions are often initiated profusely but are restricted in size, simulating an intensive hypersensitive response (HR) (Dangl and Mcdowell 2006) while in propagative mimics, lesions are relatively scarce, but then often expand

uncontrollably to kill the entire leaf and even the entire plant (Lorrain et al. 2003).

Lesion mimic mutants assume significance from twin perspectives: they help us in understanding an important phenomenon called programmed cell death (PCD); and may provide fundamentally different choice of unconventional sources of resistance in a crop breeding program that is likely more durable and broad-spectrum in scope. The recent genetic and molecular data in a wide variety of crops suggest that cell death in plants associated with HR and defense response is genetically programmed. Lesion mimic mutants are powerful tools to unravel the genetics of cell death, HR and their relationships to development. Since lesions produced by most of these mutants resemble HR, it was proposed that disease resistance and defense-related genes are involved in the formation of lesion mimics (Greenberg et al. 1994; Hu et al. 1996; Johal et al. 1995; Pryor 1987). The fact that appearance of lesions in many cases is accompanied by constitutive expression of markers associated with pathogen infection such as accumulation of auto-fluorescent phenolic compounds, production of reactive oxygen intermediates (ROI) and expression of many PR (pathogenesis-related) proteins supported this line of thinking (Hu et al. 1996). However, subsequent experiments have revealed that lesion mimic phenotypes may result from perturbations in pathways that are not necessarily involved in defense responses (Hu et al. 1998; Yamanouchi et al. 2002). As mentioned earlier, lesion mimics that display enhanced resistance and/or defense response without any negative agronomic traits may prove to be a good alternative to conventional 'R' genes in crop breeding programs, which break down often due to a matching evolution in the pathogen. Since most of the lesion mimics represent severe mis-regulation in developmental pathways, it is tempting to speculate that the corresponding evolution in the pathogen may entail enormous fitness cost, thus rendering the resistance conferred by lesion mimics more durable and broad-spectrum in nature. However, definite experimental evidences toward this hypothesis and practical applications of lesion mimics in crop resistance breeding programs other than the well-known mlo-based resistance in spring barley (Lyngkjaer et al. 2000) have not been reported till now.

A number of lesion mimic causal genes have been isolated and characterized in Arabidopsis, maize, barley and rice (Lorrain et al. 2003) and found to govern a wide array of cellular processes. LSD1 in Arabidopsis codes for a zinc-finger protein, regulating cell death at the level of transcription. LSD1 displayed propagative lesion symptoms with heightened level of resistance to virulent pathogens (Dietrich et al. 1997). ssi1, a salicylic acid (SA) insensitivity mutant in Arabidopsis that produces spontaneous HR lesions is speculated to function as a switch that modulates the cross-talk between SA and jasmonic acid/ethylene mediated defense signal transduction pathways (Shah et al. 1999). In maize, *Les22* encodes uroporphyrinogen decarboxylase which is necessary for chlorophyll biosynthesis and induces lesion resembling symptoms (Hu et al. 1998). Interestingly, perturbations in major R loci that typically belong to TIR–NBS–LRR type genes also caused lesion mimicry and enhanced resistance. *Mlo* locus in barley codes for a protein with transmembrane-spanning helices domain that is predicted to negatively regulate leaf cell death (Büschges et al. 1997). Mutations in the maize rust resistance complex *RP1* locus result in lesion mimic phenotypes and strong resistance to both maize rust isolates and non-host rusts (Hu et al. 1996). *SSI4* locus in Arabidopsis codes for a typical TIR–NBS–LRR gene and mutation at this locus leads to lesion mimicry and enhanced resistance for bacterial and oomycete pathogens (Shirano et al. 2002a, b).

A number of naturally occurring as well as induced lesion mimic mutants have been isolated in rice, which are popularly known as spotted leaf mutants (Iwata et al. 1978; Mizobuchi et al. 2002). Till date, at least 27 spl mutations have been reported of which 7 are dominant (Wu et al. 2008). Some of these spl mutants in rice show enhanced resistance and defense response to *Magnaporthe oryzae* as well as *Xanthomonas oryzae* isolates. Takahashi et al. (1999) reported eight cell death and resistant (cdr) mutants that exhibited increased resistance to an isolate of *M. oryzae* and three of them were observed to have elevated levels of the phytoalexin momilactone A and highly activated expression of two defense related genes, *PBZ1* and *PR1*. Mizobuchi et al. (2002) evaluated 14 *spl* mutants in japonica backgrounds and found enhanced resistance to blast and bacterial blight in eight mutants. Five of the mutants showed high levels of DR genes *PBZ1*, *PR1*, and *Cht3* expression, which correlated with lesion mimicry. Yin et al. (2000) reported eight *spl* mutations in IR36 background that exhibited non-race specific resistance to multiple isolates of the blast fungus, *M. oryzae* and the bacterial pathogen, *X. oryzae*. Till date, three of the spl genes have been cloned and characterized in rice. SPL7 locus encodes a heat stress transcription factor (HSF) protein which plays a critical role in making plants tolerant to cell death in response to environmental stresses such as high temperature (Yamanouchi et al. 2002). Spl11 codes for a novel protein with U box domain and six armadillo repeats and shown to possess E3 ubiquitin ligase activity indicating possible involvement of ubiquitination in plant cell death and defense response (Zeng et al. 2004). A point mutation in SPL11 locus results in premature stop codon in the protein and leads to lesion mimicry as well as broad-spectrum resistance to blast and blight pathogens in rice. Recently,

through modified activation tagging, SPL18 locus was cloned and found to code for an acyltransferase protein (Mori et al. 2007). The dominant *Spl18* mutant genotype showed up-regulation of transcription of genes for PR proteins, accumulation of momilactone A and sakuranetin and enhanced blast resistance.

Other than naturally occurring spl mutants, tissue culture-induced reverse genetic resources also act as source of lesion mimic mutants in rice. Tissue culture-induced mutations have been widely reported and seem to be ubiquitous in crop plants (Hirochika 1997, 2001). Although tissue culture-induced mutations have been used as a source of plant improvement, relatively little is known about the molecular basis. One possible mechanism is the activation of transposable elements (Larkin and Scowcroft 1981). Considering the frequency of transposition during tissue culture, *Tos17* was proposed to be involved in tissue culture-induced mutations in rice. Analysis of the target sites of Tos17 and regenerating plants with Tos17 insertions in phytochrome A and a receptor kinase like protein provided direct evidences for its involvement during tissue culture mutations (Hirochika et al. 1996). Although gene tagging with Tos17 is a powerful strategy, relatively low tagging efficiency (5–10%) has indicated involvement of mechanisms other than Tos17 insertion such as point mutations (Hirochika 2001; Agrawal et al. 2001). In this study, we systematically evaluated a large number of lines from Tos17 mutant panel developed and maintained at National Institute of Agrobiological Sciences (NIAS), Tsukuba, Japan for their reaction to three different blast (*M. oryzae*) races and identified a lesion mimic mutant line, NF4050-8 which showed lesion mimic symptoms similar to spl5 mutation with elevated levels of resistance to all the three races. Through a modified, nested AFLP procedure and southern hybridization experiments using a small set of recessive mimic individuals of a segregating population (NF4050-8 × CO39), we demonstrate here that the lesion mimic phenotype in NF4050-8 is not due to Tos17 insertion but could be due to a point mutation acquired during tissue culture regeneration. Genetic analysis and preliminary mapping of the causal locus in NF4050-8 along with spl5 population identified an overlapping genomic region of 13 cM on short arm of chromosome 7, suggesting that spl5 and NF4050-8 could be allelic or the causal genes are tightly linked. We further localized the lesion mimic causal locus in NF4050-8 to a 35 kb genomic interval, in which seven novel ORFs were identified. Expression profiling of NF4050-8 and spl5 genotypes using microarray and real-time RT PCR revealed a possible activation of WRKY45 mediated defense signaling pathway (Shimono et al. 2007), downstream of SA but independent of NH-1, in NF4050-8 and spl5.

Materials and methods

Plant materials, DNA extraction and blast screening system

NF4050-8 is a rice line identified from the Tos17 mutant panel at NIAS, Tsukuba, Japan, which produces characteristic lesions as described in the results section. NF4050-8 exhibited moderate to strong resistance response to three different races of *M. oryzae* pathogen. Two F_2 populations were developed viz., NF4050-8 × CO39 and spl5 × Kasalath with 162 and 695 individuals, respectively, for inheritance analysis and coarse mapping of the causal genes. Subsequently, NF4050-8 × CO39 was selected for further fine mapping and a large population of 950 F_3 plants was produced from a single F_2 plant that produced progenies which segregated for lesion mimic symptom in 1:3 ratio. For fine mapping and identification of candidate gene, a further large population of 3,821 F4 plants was produced from 5 F_3 plants that are heterozygous for the flanking marker interval.

DNA was extracted from leaves approximately 2 cm in length from 1- to 2-week-old rice seedlings according to a rapid and high throughput CTAB method developed previously in our lab (Xu et al. 2005). Large-scale DNA extraction of around 5 μg from selected recombinant plants (from approximately 1 g of fresh weight tissue) was obtained using an automated nucleic acid isolation system, Kurabo NA 2000.

Blast resistance reaction of different mutant lines from Tos17 mutant panel was evaluated specifically for three *M. oryzae* races viz., Ina 168 (101.0), Kyu 9439013 (047.0) and IW 81-04 (437.1) under green house conditions. Green house diagnosis of resistance was done according to an innovative, high throughput semi-natural inoculation system (Xu et al. 2008) with controlled environmental conditions such as 17–27°C day/night temperature with a day length of 14 h supplemented with fluorescent light during the winter. In brief, 2- to 3-week-old seedlings in special seedling mats were covered in a tent along with an infected mat as a source of *M. oryzae* spores at the center of a wooden pool that accommodated around nine seedling mats. Daily temperature fluctuation of 5–7°C was important to secure sufficient dew formation in the night. After inoculation, the tent was removed and seedlings were grown in the same conditions for a further 2–3 weeks to allow the symptoms to develop in intensity. The inoculated plants were evaluated for resistance reaction on a scale of 0–10 according to the manual developed by Hayashi (2005).

AFLP and southern analysis

The basic principle of AFLP assay used in this study is according to Vos et al. (1995) but with the following

modifications to suit our requirements. We designed a nested AFLP procedure in which the genuine Tos17 specific fragments were filtered in three successive PCRs using primers that are internal and specific to LTR (long terminal repeat) region of Tos17 element. The genomic DNA (150 ng/ul) was digested with *Eco*R1 (20 U/µl) and *Msp*I (20 U/µl) (BioLabs Inc, New England) (*Msp*I does not have restriction sites within the LTR region of Tos17) in a reaction volume of 15 µl with 1× Not I preservation buffer (10 mM Tris–HCl, pH 7.5, 100 mM KCl, 1 mM DTT, 0.1 mM EDTA, pH 8.0, 0.01% BSA, 0.15% Triton X-100, 50% glycerol), briefly mixed and incubated at 37.0°C for 3 h. Five microliters of the digestion solution were mixed with 1 µl *Eco*RI adapter (5 pmol/ml), 1 µl *Msp*I adapter (50 pmol/ml), 1 µl 10× ligation buffer and 28 U of T4 DNA ligase (TaKaRa) in a total of 10 µl of reaction volume and incubated at 37.0°C overnight. This digestion–ligation solution was diluted tenfold in 0.1× TE buffer and used for pre-selective amplification. Pre-selective amplification was conducted in 25 µl reaction volume containing 2.5 µl diluted adaptor-ligated DNA, 1 µl tail-3 Tos17 primer (specific to the LTR of Tos17) (5 ng/µl), 1 µl *Msp*I specific primer (30 ng/µl), 2 µl 2.5 mM dNTP each, 2.5 µl ExTaq buffer and 0.5 U ExTaq DNA polymerase (TaKaRa). The PCR profile was 94.0°C for 30 s, 56.0°C for 1 min, 72.0°C for 1 min and 20 cycles with a 10 min final extension at 72°C. The PCR products were diluted 100-fold in 0.1× TE buffer and stored at −20.0°C until further use. Selective amplification was performed in 5 µl reaction volume containing 2.45 µl diluted pre-amplification products, 0.5 µl tail-2 Tos17 specific primer (7 ng/µl) and 1.125 µl *Msp*I primer (7 ng/µl), 0.4 µl 2.5 mM dNTP each, 0.5 µl ExTaq buffer and 0.025 U ExTaq DNA polymerase (TaKaRa). The touchdown PCR profile was 1 cycle at 94.0°C for 30 s, 68.0°C for 30 s and 72.0°C for 60 s, 17 cycles with the annealing temperature reduced 0.7°C/cycle, and 23 cycles with an annealing temperature of 56.0°C and with final extension at 72.0°C for 10 min. The selective amplification PCR was repeated with diluted (1/100) template using tail-1 Tos17 specific primer. 5 µl of PCR samples were mixed with 1 µl loading buffer (0.25% xylene cyanol, 0.25% bromophenol blue, 1 mM EDTA, pH 8.0, 40% glycerol) and separated using the High Efficiency Genome Scan (HEGS) running system. The gels were run in 1× Tris–glycine buffer (25 mM Tris–HCl, pH 8.3, 1.92 M glycine) at 100 V for 80 min followed by 350 V for 4 h and stained in Vistra Green dye solution (Amersham Pharmacia Biotech) for 10–20 min, washed in water/75% EtOH for 5–10 min and scanned in FluorImager 575 (Molecular Dynamics, Amersham Pharmacia Biotech). The bands were scored manually.

For the southern analysis, total genomic DNA (500 ng) was digested with *Xba*I over a period of 18 h and separated on a 0.8% (w/v) agarose gel. Lambda/*Hin*dIII was used as the marker and Nipponbare/*Xba*I as the reference (control) lane. After the electrophoresis, gels were blotted on to Hybond N nylon membrane (Amersham Pharmacia Biotech) and denatured for 5 min with an alkaline solution (1.5 M Nacl and 0.5 M NaOH) and washed with 2× SSC thoroughly. The membrane was prehybridized with Church–Gilbert hybridization buffer (Church and Gilbert 1984) for 3 h at 65°C. Probe (Tos17) was added directly to the hybridization buffer, and hybridization was continued for 18 h. Probes were labeled by Multiprime DNA labeling system (Amersham, Buckinghamshire, UK) using [α-^{32}P]dCTP (Amersham), and non-incorporated nucleotides were removed by spin chromatography. The hybridized membrane was washed with 2× SSC and 0.1% (w/v) SDS at the same temperature for 1 h, and exposed to an X-ray film (Kodak, Tokyo) for 18 h.

SSR and SNP marker analysis

Primers for SSR markers were synthesized based on Gramene database (http://www.gramene.org/microsat). SNPs were detected by aligning the reference japonica (Nipponbare) (http://www.rgp.dna.affrc.go.jp) and indica (93-11) (http://www.rise.genomics.org.cn) sequences at the target location. Primers were designed for SNP markers using primer3 software. The uniqueness of each primer in the rice genome was confirmed by BLAST analysis. A gel based, low cost, high throughput SSCP (single strand conformational polymorphism)–SNP genotyping assay was earlier developed in our lab (Xu et al. 2009), which was extensively used in the present investigation. As far as possible, the SNP was positioned in the center for SSCP electrophoresis. Amplifications were performed with MicroAmp™ optical 384-well reaction plate and the GeneAmp® PCR system 9700 (Applied Biosystems, USA) with the following parameters: 94.0°C for 2 min; 30 cycles at 98.0°C for 10 s, optimized annealing temperature for 20 s, and 72.0°C for 30 s; and a final extension at 72.0°C for 10 min. Each tube of 5 µl PCR reaction contained 0.5 µl template DNA, 0.2 U of TAKARA Ex *Taq*™, 100 µM of each dNTP, 1× TAKARA Ex *Taq*™ buffer, and 0.5 µM primers. After the addition of 0.5 µl 10× loading dye (0.25% bromophenol blue, 0.25% xylene cyanol, 50% Glycerol), for SSCP–SNP analysis, PCR products were denatured by heating to 96.0°C for 5 min and on ice for 2 min. The denatured products were kept on ice until loaded onto SSCP gel at 4.0°C. Single-band PCR fragments were confirmed on 1% agrose gels and directly sequenced (using the same F and R PCR primers) with an ABI BigDye® Terminator v3.1 Cycle Sequencing Kit and ABI 3100 DNA sequencer (Applied Biosystems, Foster City, CA) to confirm the SNPs.

HEGS (high efficiency genome scanning) (NIHON EIDO) is a high throughput polyacrylamide gel electrophoresis system designed in our laboratory especially for construction of high density maps of targeted loci in model species in legumes and cereals. The system is equipped with two sets of 24.5 × 26.5 cm glass plates, each accommodating a 1 mm thickness gel with a provision to run 100 lanes. There are four gels in a single unit and one technician can handle two units at a time enabling analysis of 800 samples in a single run. The gel consists of two kinds of non-denaturing gel matrices. 5% stacking gel containing 125 mM of Tris–HCl (pH 6.8) and 8–13% running gel containing 375 mM of Tris–HCl (pH 8.8). The running buffer consisted of 25 mM Tris and 192 mM of glycine. The PCR products were loaded with 8 or 16 channel syringe loader. The samples are electrophoresed at 200 V for 1 h (for stacking gel) and then at 400 V for 16–20 h (for 13% running gel) at 4–8°C controlled by UA-100 temp-controller (EYELA, Tokyo) with buffer cooler jackets (for SSCP–SNP analysis). After electrophoresis, the gels were stained with Vistra Green (Amersham Biosciences, Uppsala, Sweden) and scanned by a fluorescence scanner (Fluorimager 575, Amersham Biosciences, Piscataway, USA) or using a high-resolution digital camera (>5 M pixels) with UV filters (Xu et al. 2009; Kawasaki and Murakami 2000).

Gene annotation

Open reading frames (ORFs) and potential exon/intron boundaries were predicted for the 35 kb sequences delimited by the fine mapping strategy using the Rice-GAAS program (http://ricegaas.dna.affrc.go.jp), which integrates a number of other prediction softwares for coding regions (GENSCAN, RiceHMM, FGENESH, MZEF), splice sites (SplicePredictor), homology search analysis (Blast, HMMER, ProfileScan, MOTIF), tRNA gene prediction (tRNAscan-SE), repetitive DNA analysis (RepeatMasker, Printrepeats), signal scan search (Signal Scan), protein localization site (PSORT), and program of classification and secondary structure prediction of membrane proteins (SOSUI). Interpretation of the coding region in Rice-GAAS is fully automated and gene prediction is accomplished without manual evaluation and hence following operations were done to confirm the annotation results. The potential identities of predicted coding sequences were found by searching against the non-redundant protein and DNA databases and against the species specific (*Oryza sativa*) EST databases at the National Center for Biotechnology Information (http://www.ncbi.nlm.nih.gov), Gramene (http://www.gramene.org) and The Institute for Genomics Research (TIGR) (http://www.tigr.org) (currently known as J. Craig Venter Institute, http://www.jcvi.org) using the BLASTN and BLASTP programs (Altschul et al. 1997). The rice repeat database http://www.tigr.org/tdb/e2Kl/osa/blastsearch.shtml was searched to locate repeats within the sequences and positive hits were classified as either retrotransposons, transposons or miniature inverted repeat transposable elements (MITE).

Microarray analysis

Total RNA from leaves was isolated using the RNeasy Plant Minikit (Qiagen, Valencia, CA) and used for synthesis of labeled cRNA target. Microarray experiments were conducted as described in Kottapalli et al. (2007). The RNAs were extracted from leaves of NF4050-8 and Nipponbare 50 days after sowing, when the appearance of lesion mimic symptom in NF4050-8 was conspicuous and in progressive stage. In brief, labeled cRNA from leaf tissue of mutant was hybridized with wild type in two biological replicates. For detection of significant differentially expressed genes, each slide image was processed by Agilent Feature Extraction software (version 9.1). This software measured Cy3 and Cy5 signal intensities of whole probes. Since dye bias tends to be signal intensity-dependent, probe sets for dye normalization were selected by rank consistency. Normalization was done by locally weighted linear regression (LOWESS). Ratios were log-transformed and significance values (*P* value) were calculated based on a propagate error model and universal error model. In this analysis, the threshold of significant differentially expressed genes was determined with a *P* value $\leq$0.05 (*P* value is a measure of the confidence that the feature is not differentially expressed). Low-quality spot data generated due to artifacts were eliminated prior to data analysis. Processed intensities from feature extraction analysis were imported into the TIGR Multiexperiment Viewer software (MEV 4.1) and significant genes at a *P* value of $\leq$0.05 and more than threefold difference in expression were defined as differentially expressed. The Gene Ontology functional annotation tool Blast2GO (Conesa and Götz 2008) was utilized to assign GO ids, enzyme commission numbers, and mapping to Kyoto Encyclopedia of Genes and Genomes (KEGG) pathways. The Blast2GO tool also enabled statistical analysis related to over-representation of functional categories based on a Fisher exact statistic methodology. The microarray data presented in this paper was deposited in the NCBI Gene Expression Omnibus and accessible through the series accession number GSE17791.

Real-time quantitative PCR

RT-PCR was performed with 2 μg of total RNA treated with DNase I (Invitrogen). Reverse transcription was done using SuperScript III RNase H^- (Invitrogen) and oligo$(dT)_{23}$ primers (Sigma-Aldrich). PCR was performed

using cycles of 94°C for 30 s, 55°C for 30 s, and 72°C for 1 min, followed by a final extension at 72°C for 7 min. Quantitative RT-PCR was run on a Thermal Cycler Dice TP800 system (Takara Bio) using SYBR premix Ex Taq mixture (Takara) with cycles of 95°C for 5 s and 60°C for 30 s. *Rice ubiquitin 1* (*Rubq1*; AK121590) was used as an internal standard. Primers for RT-PCR of WRKY45: F: CG GGTAAAACGATCGAAAGA and R: TTTCGAAAGCG GAAGAACAG. Primers for RT-PCR of PR 1b: F: ACGG GCGTACGTACTGGCTA and R: CTCGGTATGGACC GTGAAG. These primer sets were tested by dissociation curve analysis and verified for the absence of nonspecific amplification.

Results

Isolation of a lesion mimic mutant genotype, NF4050-8 from a *Tos17* mutant library collection available with NIAS, Japan

We screened several lines from *Tos17* rice mutant panel for their reaction to infection with three blast races viz., Ina 168 (101.0), Kyu 9439013 (047.0) and IW 81-04 (437.1) under green house conditions. Koshihikari and Kahei were used as susceptible and resistant control, respectively, in all the blast screening experiments. Two mutant lines, NF4050-8 and NF4050-12 consistently showed moderate degree of resistance to all the three races used in the study. A set of spl mutant genotypes were also included in the screening experiments and interestingly, the resistance response of NF4050-8 and NF4050-12 mutant lines was more or less similar to spl5 with respect to all the three blast races (Fig. 1). Both these mutant lines produced small brown lesions, when grown under normal, uninfected conditions. The lesions initially appear as tiny brown spots on the tip of the young leaves early in the growth stage (after 20−30 days after sowing) and gradually gain prominence at flowering and intensify toward maturity. In the older plants, the lesions coalesce and form brown smudges covering almost the entire leaf surface (Fig. 2) in most of the leaves. The onset and severity of lesions in NF4050-8 and NF4050-12 varied depending on whether the plants were grown under green house or field conditions. When grown in field conditions, the lesion mimic symptom was more conspicuous and later than that of plants grown under green house environment.

Inheritance and genetic analysis

We selected NF4050-8 and spl5 for detailed genetic and molecular analyses. We developed two segregating F_2 populations viz., NF4050-8 (japonica) × CO39 (indica)

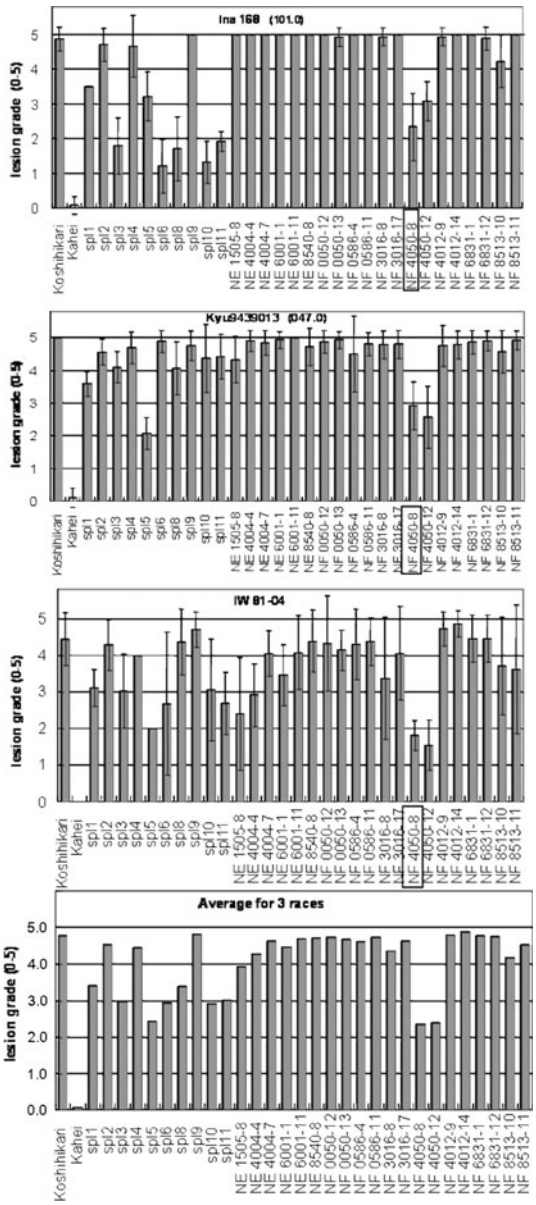

Fig. 1 Evaluation of Tos17 mutant panel lines along with a set of spl genotypes for reaction to three different blast races

and spl5 (japonica) × Kasalath (indica) in 2005. The F1 plants of both the crosses did not show lesion mimic symptom indicating that the causal genes are most likely recessive in nature. Under field conditions, out of the 162 F_2 plants of NF4050-8 × CO39, 18 plants showed the lesion mimic symptoms (Chi-square value for 1:15 ratio is 6.59, $P < 0.05$), while in spl5 × Kasalath F_2 population, 32 plants expressed lesion mimic symptoms out of a total of 695 plants (chi-square value for 1:15 ratio is 3.19, $P > 0.05$). By combining classical and RFLP map, earlier studies with japonica × japonica crosses have reported that *spl5* phenotype is governed by single recessive gene on the short arm of chromosome 7 (Yoshimura et al. 1997).

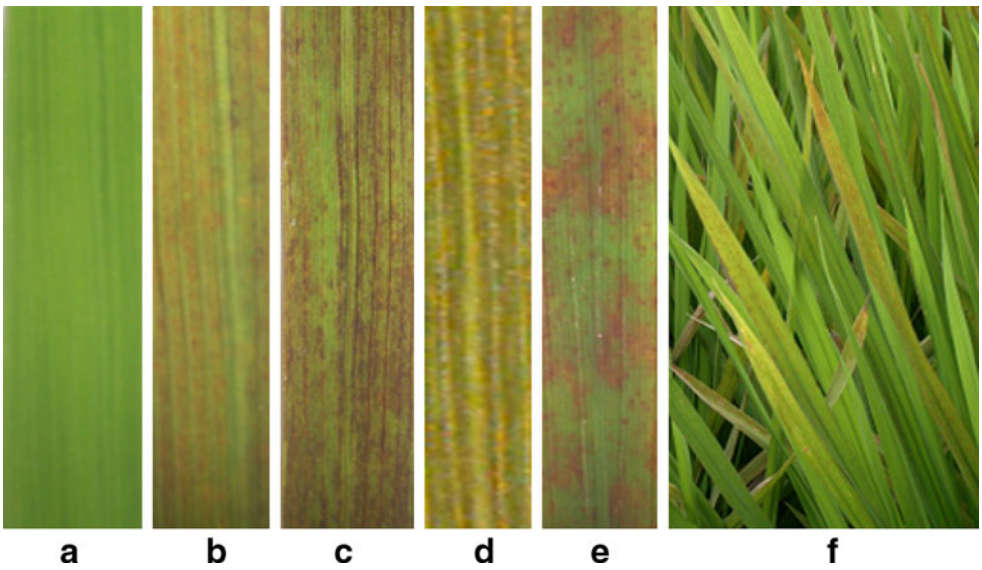

Fig. 2 Lesion mimic symptoms of spl5 and NF4050-8. **a** Nipponbare (control); **b**, **c** spl5 during early and later stages of lesion appearance; **d**, **e** NF4050-8 during early and later stages of lesion appearance and **f** NF4050-8 plant under field grown conditions

This led us to the conclusion that though the underlying factor for lesion mimic symptom is single recessive gene, in japonica × indica crosses, there could be a dominant suppressor factor regulating the expression of lesion mimic symptom as in NF4050 × CO39 and spl5 × Kasalath crosses. However, test of homogeneity of segregation ratios ($P = 0.0015$) between the two crosses confirmed that these crosses behave differently for the segregation of lesion mimic phenotype. It is possible that the second Mendelian factor may be independent of the first one in spl5 × Kasalath, but linked to the causal lesion mimic locus in NF4050-8 × CO39.

Mutation in NF4050-8 is not due to *Tos17* insertion and could be due to nucleotide change(s) acquired during tissue culture regeneration

Tos17 is activated by tissue culture and inactivated again in regenerated plants in rice (Hirochika et al. 1996). Gene tagging with *Tos17* has proved to be an effective tool for cloning a number of genes in abscisic acid biosynthesis in rice (Agrawal et al. 2001). However, fundamental problems with *Tos17* mutant collection include relatively low tagging efficiency and variations that arise due to tissue culture regeneration processes other than *Tos17* insertion, which account for significant proportion of the mutants. We designed a modified nested AFLP procedure to determine whether NF4050-8 contains a *Tos17* insertion in the target locus responsible for lesion mimic symptom using a set of 18 recessive lesion mimic F_2 plants identified from field evaluation of the NF4050-8 × CO39 population. *Tos17* is 4.3 kb long, and carries two identical 138 bp LTRs (Long Terminal Repeat). We searched for restriction endonucleases that do not have restriction sites inside the LTR region of *Tos17* and identified two enzymes viz., *Msp*I and *Hha*I (Fig. 3a). Genomic DNA was digested with *Msp*I and *Eco*RI followed by selective amplification using *Msp*I specific primers and *Eco*RI adaptors. Since there are numerous *Tos17* analogs in rice genome, we used a nested AFLP procedure wherein three primers specific and internal to LTR region of Tos17 were used to filter the genuine Tos17 sequences in three successive PCRs. Nipponbare has two copies of Tos17 and is the base material from which NF4050-8 was regenerated through tissue culture process. The half-nested AFLP (2nd PCR) produced comparatively better results (Fig. 3b) and none of the candidate bands that showed clear polymorphism among the parental lines viz., NF4050-8, CO39 and Nipponbare co-segregated with the lesion mimic phenotype in recessive lesion mimic F_2 individuals of NF4050-8 × CO39. The third PCR (full-nested) profile (data not shown) identified two candidate bands that are polymorphic among the parental lines and specific to NF4050-8 but did not co-segregate with the recessive lesion mimic phenotype of F_2 individuals from NF4050-8 × CO39. To confirm and validate these AFLP results, we conducted further a southern experiment using Tos17 specific probes. DNA gel blot analysis was performed with XbaI restricted genomic DNA of parental lines along with 14 recessive lesion mimic F_2 plants from NF4050-8 × CO39 population using Tos17 specific sequences as probe (Fig. 3c). One polymorphic fragment could be observed between NF4050-8 and CO39/Nipponbare, which however did not co-segregate with the lesion mimic phenotype of recessive lesion

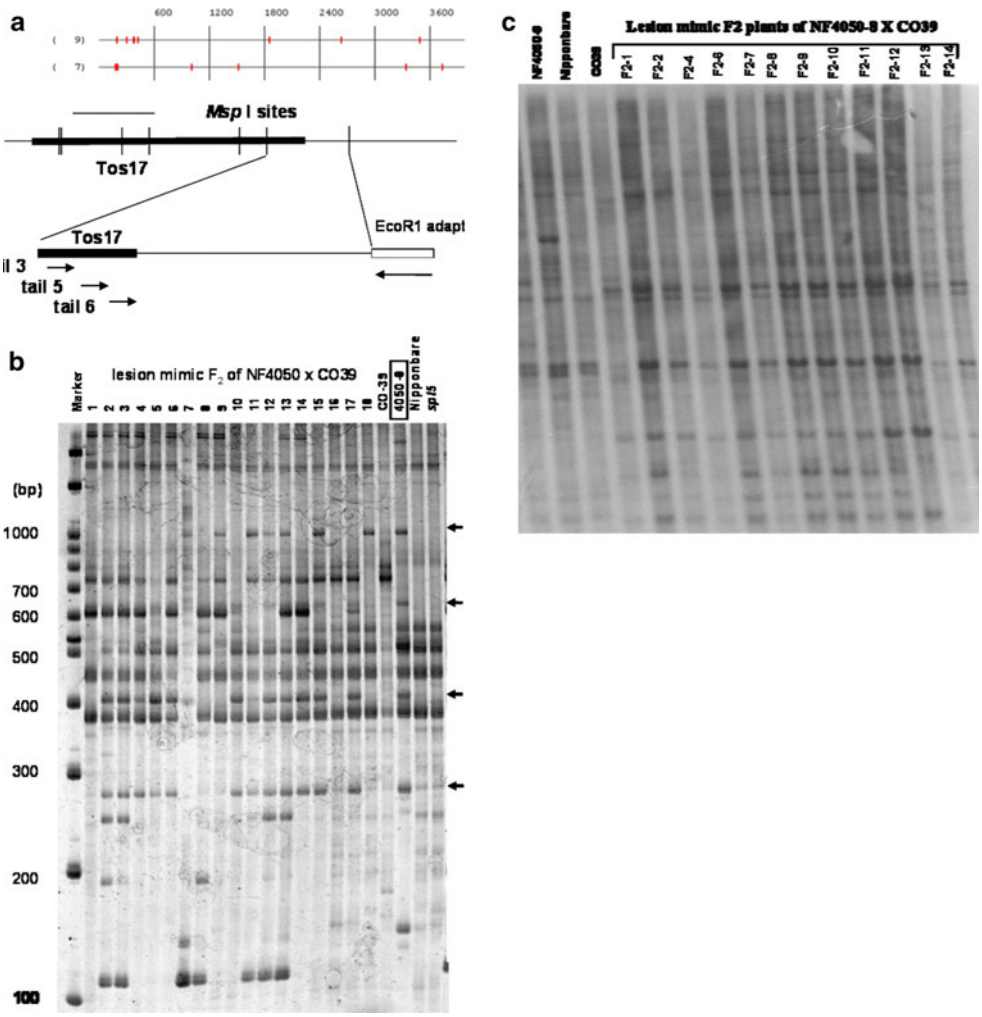

Fig. 3 **a** Selection of restriction enzymes that do not have restriction sites within the 130 bp LTR region of Tos17 (4.3 kb) for the nested AFLP experiment. **b** Modified half-nested AFLP of recessive F_2 lesion mimic individuals of NF4050-8 × CO39 using Tos17 specific primers located within LTR region. Polymorphic candidate bands between parental lines, NF4050-8 and Nipponbare/CO39/spl5 are indicated with *black arrows*. None of the candidate bands co-segregated with all the recessive lesion mimic F_2 plants. **c** DNA gel blot (southern) analysis of XbaI restricted genomic DNA of recessive lesion mimic F_2 plants of NF4050-8 × CO39 with Tos17 probes. The polymorphic fragment indicated with the *arrow* mark however did not co-segregate with the lesion mimic phenotype

mimic F_2 plants identified from NF4050-8 × CO39 reinforcing the earlier results of nested AFLP that the lesion mimic phenotype of NF4050-8 is most likely due to other nucleotide variations acquired during tissue culture regeneration process rather than due to *Tos17* insertion per se.

The causal gene in NF4050 (spl^{NF4050}) could be allelic or tightly linked to *spl5* locus in rice

To ascertain a rough estimate of map positions of spl5 and NF4050-8 causal gene, recessive class analysis using lesion mimic individuals identified from two segregating populations, spl5 × Kasalath (32 lesion mimic F_2 plants) and NF4050-8 × CO39 (18 lesion mimic F_2 plants) was performed with SSR markers distributed evenly on chromosome 7 of rice (Table 1). The recombination frequency (*c* value) between a marker and the targeted lesion mimic locus was calculated by assuming that all the lesion mimic F_2 plants from both the crosses were recessive at the lesion mimic locus. The genetic distances calculated based on the specific segregating populations developed in this study largely coincided with the established map locations of the SSR markers on IRMI2003 map (Fig. 4). Small discrepancies with SSR markers located right of NF4050-8 causal gene based on NF4050-8 × CO39 map might have been due to smaller population size or segregation distortion, which is frequently observed in rice (Zhang et al. 1994). The identified candidate region on chromosome 7 for spl5 and NF4050-8 causal gene using two independent segregating populations largely overlapped and was defined by RM7479 (left) and RM8037 (right). RM6574 (38.4 cM) co-segregated with the lesion mimic phenotype in NF4050-8 × CO39 population, while it was found to be non-polymorphic in spl5 × Kasalath cross. RM8247 (41.7 cM) co-segregated with the lesion mimic phenotype in spl5 × Kasalath cross, while one heterozygous recombinant (with the lesion mimic phenotype) was detected in the field evaluated NF4050-8 × CO39 F_2 population. In addition to the above-said F_2 populations, a set of 92 recessive lesion mimic F_3 plants identified from green house evaluation of heterozygous F_2 plants that segregated for lesion mimic symptom was analyzed with the same set

Table 1 Recessive class analysis using SSR markers from chromosome 7 of rice in two segregating F_2 populations of spl5 × Kasalath and NF4050-8 × CO39

Name of the marker	Genetic map location on chr. 7[a] (cM)	Physical map location on chr. 7[a] (Mb)	Spl5 × Kasalath, F_2 (field evaluation)					NF4050-8 × CO39, F_2 (field evaluation)					NF4050-8 × CO39, F_3 (green house evaluation)				
			No. of spl5 homo	No. of Kasalath homo	No. of Hetero	Total no. of mimic plants	C value[b] (cM)	No. of NF4050 homo	No. of CO39 homo	No. of Hetero	Total no. of mimic plants	C value[b] (cM)	No. of NF4050 homo	No. of CO39 homo	No. of Hetero	Total no. of mimic plants	C value[b] (cM)
RM6652	2.5	0.579	15	6	10	31	35.5	Not polymorphic					Not polymorphic				
RM6047	3.9	0.741	15	4	12	31	32.3	10	1	7	18	25.0	60	6	28	92	20.8
RM5711	24.0	3.140	20	2	9	31	20.1	Not polymorphic					Not polymorphic				
RM7479	31.0	4.133	28	–	3	31	5.8	15	–	2	17	5.9	84	–	5	89	2.8
RM21103	–	4.160	28	–	3	31	5.8	15	–	2	17	5.9	90	–	2	92	1.1
RM6574	38.4	4.681	Not polymorphic					17	–	–	17	0.0	91	–	–	91	0.0
RM8247	41.7	5.728	31	–	–	31	0.0	16	–	1	17	2.9	88	–	–	88	0.0
RM21196	–	6.080	Not polymorphic					15	1	1	17	8.8	80	2	10	92	6.5
RM1253	44.4	6.966	29	–	2	31	3.2	Not polymorphic					Not polymorphic				
RM8037	50.0	14.54	28	–	3	31	4.8	14	1	2	17	11.7	66	4	22	92	16.3
RM6449	53.0	15.41	28	–	3	31	4.8	15	1	2	18	11.1	63	5	24	92	18.5
RM6767	60.8	17.47	25	–	7	32	10.9	10	3	4	17	29.4	51	9	30	90	26.6
RM3404	70.0	20.11	24	–	7	31	11.3	9	2	3	14	25.0	48	10	34	92	29.4
RM1279	75.0	21.61	Not polymorphic					11	1	6	18	22.2	44	10	38	92	31.5

[a] Genetic map location of SSR markers is based on IRMI2003 map. The positions of the SSR markers are reported relative to RFLP and STS markers on the JRGP RFLP 2000 map. Physical location of SSR markers is based on 'Gramene Annotated Nipponbare Sequence 2006'

[b] *c* value (the genetic distance between the gene and marker loci) calculated as below $N1 + (N2/2)/N \times 100$, where $N1$ is no. of homozygous recombinants, $N2$ is no. of heterozygous recombinants and N is total number of plants analyzed (Zhang et al. 1994)

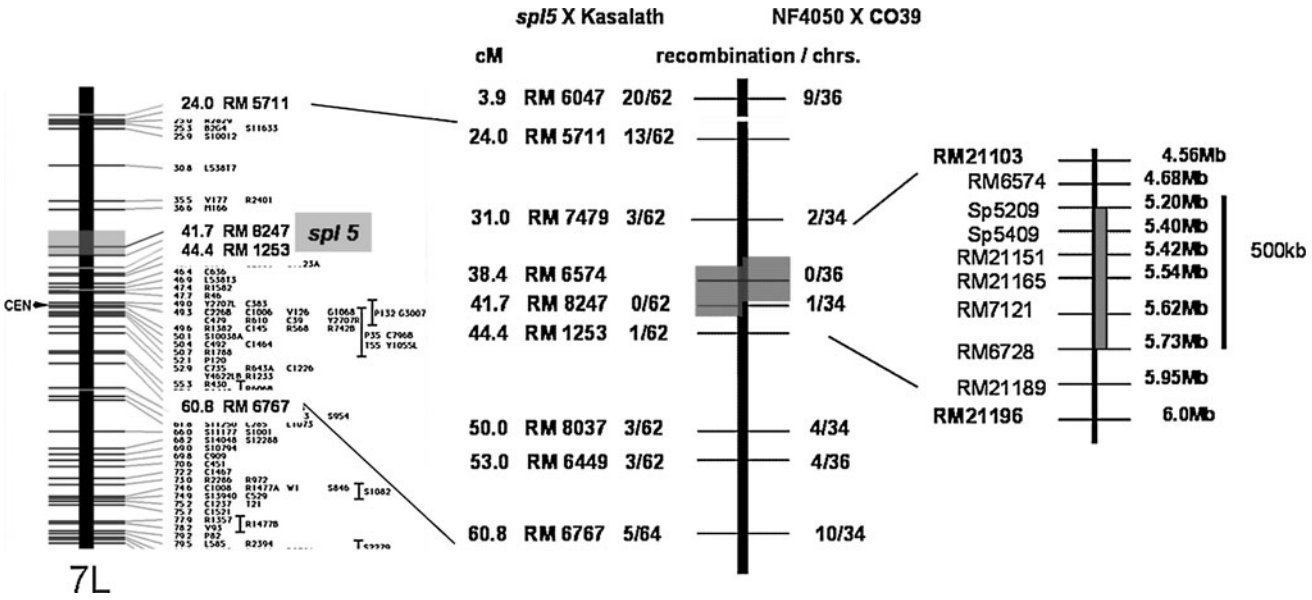

Fig. 4 Molecular mapping of lesion mimic locus in two F_2 populations, spl5 × Kasalath and NF4050-8 × CO39 to an overlapping region of 13 cM on long arm of chr. 7 and subsequent localization to 500 kb region using 950 F_3 plants of NF4050-8 × CO39

of SSR markers located on chromosome 7. The genetic map constructed based on green house evaluation of the lesion mimic symptom was largely in agreement with the genetic map of field evaluated F_2 plants of NF4050-8 × CO39 population. These results taken together suggest that the causal lesion mimic locus in NF4050-8 is either allelic or tightly linked with the spl5 locus on short arm of chromosome 7.

Identification of $F_{2:3}$ lines from NF4050-8 × CO39 that segregate for lesion mimic symptom in 1:3 ratio without the influence of indica factor

In order to fine map and proceed toward identifying the candidate gene underlying the lesion mimic locus in spl5 and NF4050-8 genotypes, we searched for $F_{2:3}$ lines that segregate in '1 lesion: 3 normal' plants ratio without the influence of a second factor from indica. 17 plants were evaluated for development of lesion mimic symptom for each $F_{2:3}$ line and a total of 60 randomly selected F2 progenies from NF4050-8 × CO39 and 25 F_2 progenies from spl5 × Kasalath crosses were evaluated under green house conditions. In spl5 × Kasalath cross, we could not identify any $F_{2:3}$ progeny line that segregated in 1:3 ratio, while eight $F_{2:3}$ lines could be identified that segregate in 1:3 ratio for the lesion mimic symptom under green house conditions in NF4050 × CO39 cross. The eight green house identified $F_{2:3}$ lines were evaluated again under field conditions and one line (F2-16-14) that segregated in 1:3 ratio in an unambiguous manner was selected for developing a large mapping population toward fine mapping of the spl^{NF4050} locus.

High-resolution genetic mapping using large 1:3 segregating populations of NF4050-8 × CO39 delimits $spl^{NF4050\text{-}8}$ locus to 35 kb region on chromosome 7

A population of around 950 plants from F2-16-14 (that segregate in 1:3 ratio for lesion mimic symptom) was screened with two flanking markers viz., RM21103 (4.56 Mb) and RM21196 (6.04) with high efficiency genome scan (HEGS) system. A total of 72 recombinants were identified that contained a homozygous mutant genome (NF4050-8) fragment on one end and heterozygous fragment at the other end for the flanking marker interval, which was around 1.6 Mb on short arm of chromosome 7. The selected recombinants were evaluated for lesion mimic symptom under field conditions. 48 of the 72 recombinants showed clear lesion mimic symptom while the rest did not. The selected recombinants were further screened with internal markers physically located at regular intervals within the delimited 1.6 Mb region. The genomic regions covered by three BAC accessions viz., AP003848, AP004379 and AP005257 spanning around 350 kb region contained only two ready to use SSR markers and hence we designed a number of SSCP–SNP markers using the publicly available sequence information of japonica (Nipponbare) and indica (93-11) databases. Out of a total of 12 primer pairs designed and tested, we could generate seven successful polymorphic SNP markers in the above-mentioned interval, which produced PCR products of expected sizes in NF4050-8 and CO39 genotypes. The amplified PCR products were resolved in SSCP–PAGE gels under cold conditions of 4°C for 16 h, which helped in gel based genotyping of SNPs in several thousand samples

in a short span of time in a cost effective way. The physical placement of newly developed markers in relation to other established markers is shown in Fig. 5.

The graphical genotype, shown in Fig. 5 based on 72 recombinants and 10 marker genotypes combined with the lesion mimic phenotype information ('Yes' indicates presence of lesion mimic symptom, while 'No' indicates absence) of these recombinants identified a candidate region of around 500 kb flanked by Sp5209 (5.21 Mb) and RM6728 (5.73 Mb) markers. Within the flanking marker interval, three double recombinants were identified using the internal markers, in which two recombination events between Sp5409 and RM21165 were rare and surprisingly no single recombinants could be identified for this recombination event. With the aid of three double recombinant genotypes and their respective phenotype, the candidate region could be tentatively narrowed down to approximately 200 Kb between Sp5209 and Sp5409 markers. All the single and double recombinants were grown in the field during the following season and confirmed for the lesion mimic phenotype and segregation of the heterozygous regions within the flanking marker interval.

To increase the confidence of the fine mapping process in the absence of critical single recombination event between Sp5409 and RM21165 in the F_3 plants, a population of 3,821 F_4 plants was developed from five heterozygous F_3 plants of NF4050-8 × CO39 and screened with two flanking markers viz., RM6574 and RM21189. The primers were multiplexed in single PCR reaction and the length of the HEGS gel facilitated resolution of both the PCR products in a single gel thereby enabling 192 data points per gel or up to 1,536 data points per person per day. A total of 146 recombinants were identified between

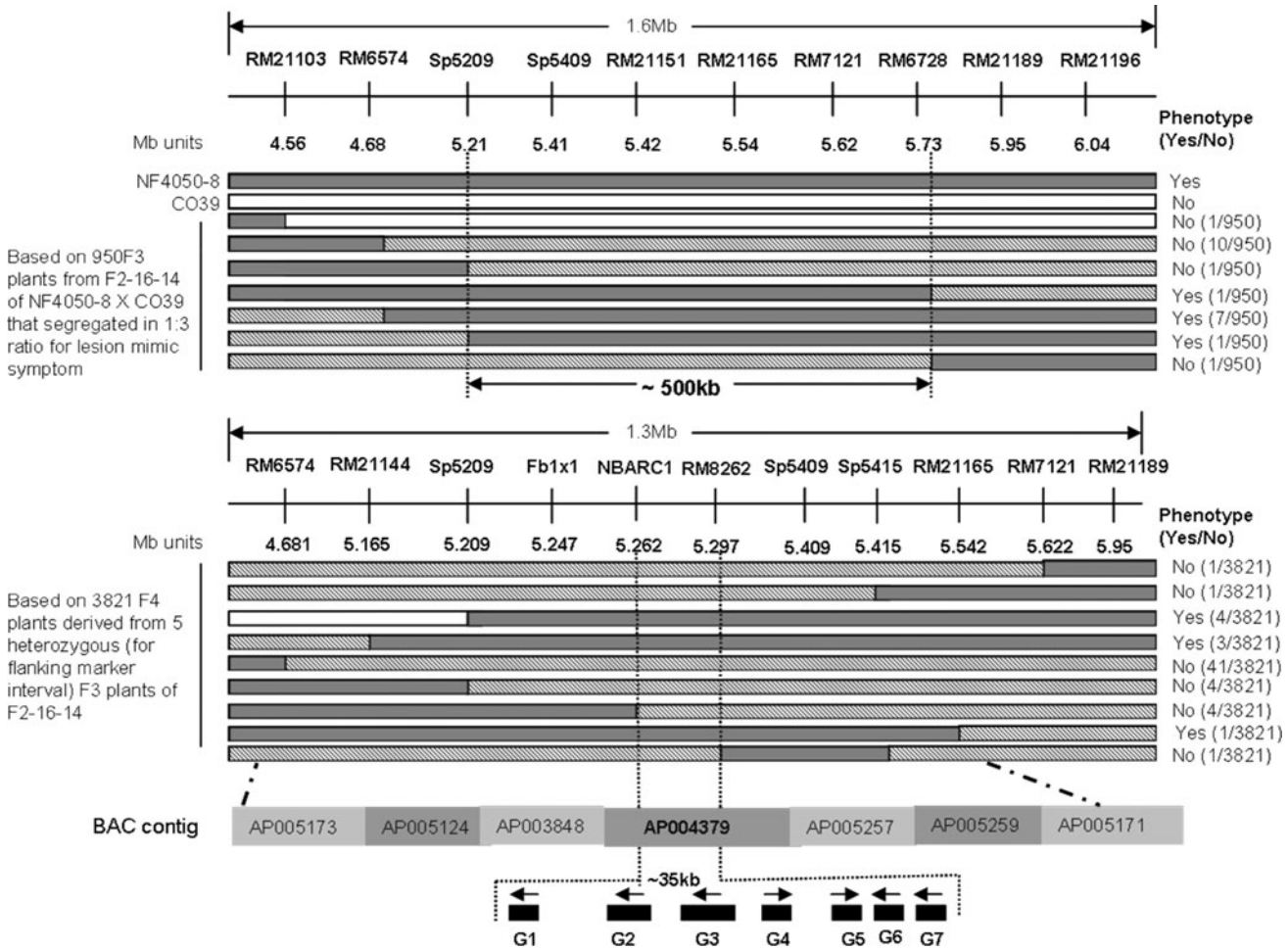

Fig. 5 Fine mapping and physical delimitation of lesion mimic causal locus in NF4050-8 to 35 kb region on BAC contig, AP004379 using critical recombinants identified from 950 F_3 and 3,821 F_4 plants of NF4050-8 × CO39. The marker distances are according to physical scale (Mb). *Black bar* represents homozygous NF4050-8 genome; *white bar* represents homozygous CO39 genome and the *hatched bar* represents heterozygous. '*Yes*' phenotype indicates presence of lesion mimic symptom while '*No*' indicates absence. *Numbers in parenthesis* indicate number of individuals identified in the respective recombinant category. The seven ORFs identified in the delimited interval are indicated according to their natural orientation on the genome

RM6574 and RM21189 that contained lesion mimic parent genome in either homozygous or heterozygous condition upstream of RM21189 and down stream of RM6574. Since the lesion mimic phenotype is recessive in expression, we selected only those individuals with the exchange of flanking marker genotypes of lesion mimic genome (NF4050-8) in homozygous and heterozygous status and phenotyped them for lesion mimic symptom expression under field conditions. Using the previously described SSCP–SNP marker development technique, a number of new polymorphic markers were developed within the flanking marker interval. With genotyping of five more SSR markers, the marker density in the targeted region was around 35–40 kb per pair of marker interval. Several classes of recombinants with precisely delimited recombination break points between each of the pair of internal markers and their respective phenotype information reconfirmed the 500 and 200 kb (with double recombinant genotype) candidate regions identified using 950 F_3 plants.

Between the two markers, Sp5209 and Sp5401, three classes of informative recombinants could be identified. The first class of recombinants comprised of eight individuals, four of them contained CO39 genome in homozygous condition upstream of Sp5209 and they expressed lesion mimic symptom clearly, while the other four plants of this recombinant class contained NF4050-8 genome in homozygous condition upstream of Sp5209 and did not express the lesion mimic symptom, confirming the candidate region to be downstream of Sp5209. The second class of recombinants with no lesion mimic phenotype consisted of four plants with recombination break point between NBARC1 (5.262) and RM8262 (5.297), containing NF4050-8 genome in homozygous condition upstream of NBARC1, which ruled out the genomic region between Sp5209 and NBARC1. The third class of recombinants had only one plant with double recombination breakpoints between RM8262 (5.297) and Sp5415 (5.415). The genomic region flanked by these two markers in this double recombinant individual was homozygous for NF4050-8 genome and did not express the lesion mimic phenotype, thus delimiting 35 kb marker interval flanked by NBARC1 (5.262) and RM8262 (2.297) as the candidate region for the $spl^{NF4050\text{-}8}$ lesion mimic locus.

The detailed analysis of recombination in the large F_3 and F_4 populations allowed us to identify some recombination cold spots in the target region (Fig. 6). Overall, the 1.3 Mb region flanked by RM6574 and RM21189 had a physical to genetic distance ratio of around 340 kb/cM, which appeared to be normal in genomic regions closer to centromere. The centromere region on chromosome 7 is estimated to be around 1.1 Mb defined by markers, C39 (11.36 Mb) and C12887S (12.54 Mb) (Wu et al. 2003). The region downstream of Sp5409 in general appeared to be recombinationally suppressed with an average physical to genetic distance ratio of more than 500 kb/cM. Similar trend is reflected in F_4 population based on analysis of 3,821 plants, in which the region flanked by RM8262 and SP5404 appeared to be most inactive for which no recombination events could be detected and the regions downstream to this had a physical to genetic distance ratio of more than 1,500 kb/cM until RM7121.

Annotation of genetically delimited 35 kb genomic interval with Rice-GAAS and Gramene

The 35 kb candidate region physically delimited by NBARC1 and RM8262 was annotated with Rice-GAAS and the results were compared with Gramene dB annotation. The annotation results were largely consensual except for two additional ORFs predicted by Rice-GAAS, which are discussed later in detail. The candidate region contained seven ORFs in all, of which, three of them were 'resistance gene related' with typical NBS–LRR signatures, one hypothetical protein similar to blight resistant RGA3 like protein, one transposable element (TE) with WRKY17 like element (predicted by Rice-GAAS), one putative DNA-directed RNA polymerase I subunit RPA1 (predicted by Rice-GAAS) and one expressed but unknown protein (Table 2). One of the resistance gene related ORFs (LOC_Os07g09920/Os07g0197500) harbored a NB–ARC domain, which had been demonstrated to be associated with cell death in animals (Van der Biezen and Jones 1998). Gene density within this region was around one gene every 6 kb, slightly lower than published predictions of one gene every 4–5 kb (Yu et al. 2002; Blair et al. 2002). The average gene size of 1.44 kb was considerably smaller than the 4.5 kb predicted earlier by Yu et al. (2002) and TIGR predictions of 2.47 kb (http://www.tigr.org/www.jcvi.org). The GC content for coding regions was around 60% on average and was higher in exons than introns. Consistent with earlier published information, variation within genes was such that most of the candidate cDNAs had higher GC content at 5′ protein coding end compared to the 3′ UTR.

Microarray analysis of NF4050-8 with Nipponbare as control

We performed microarray analysis of ~44,000 rice genes in NF4050-8 with Nipponbare as control/wild using a 60-mer oligo DNA microarray. The gene expression levels were compared using an agilent system with two biological replicates. Statistical analysis using analysis of variance false discovery rate (q value) <0.05 (Sharov et al. 2005) identified around 110 differentially expressed genes between NF4050-8 and Nipponbare (Table 3). Several

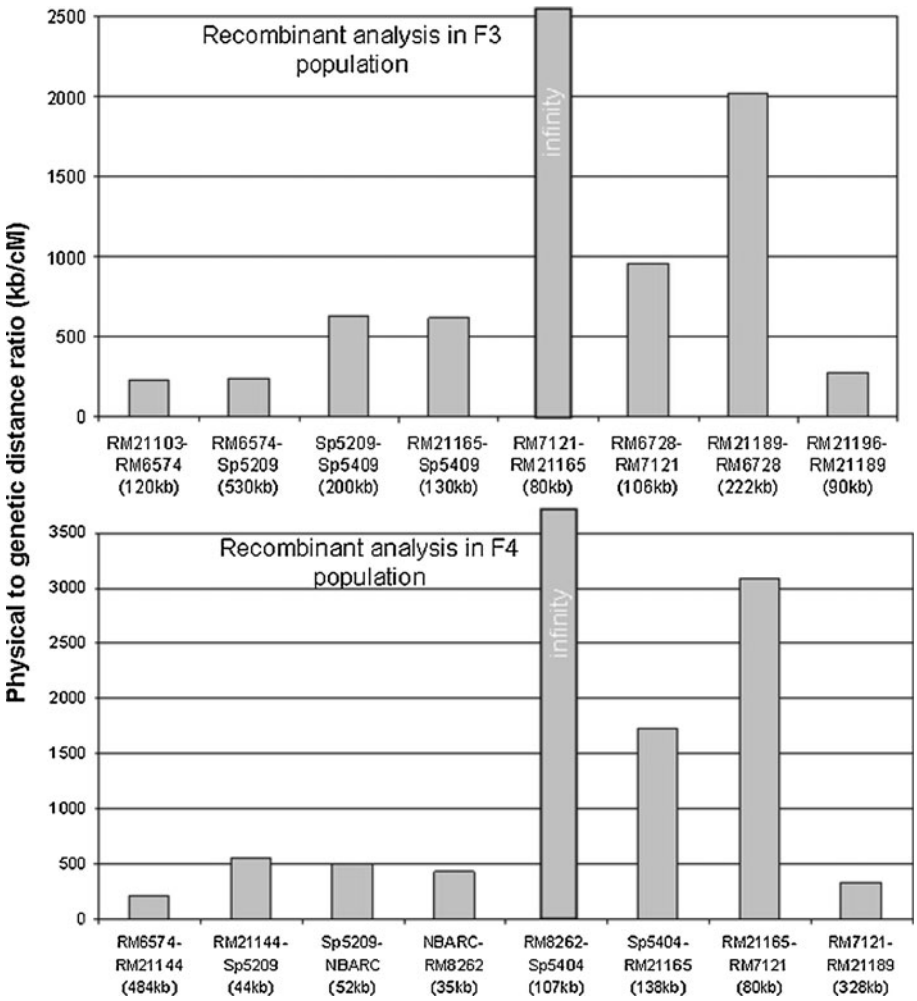

Fig. 6 Physical to genetic distance ratio (kb/cM) in the 1.3 Mb delimited interval based on F_3 and F_4 plants from NF4050-8 × CO39. Overall this centromeric region had a physical to genetic distance ratio of 340 kb/cM while the genomic region downstream of Sp5409 was found to be recombinationally suppressed (500 kb/cM) in F_3 population analysis. Similar trend was observed in F_4 population

defense/pathogenesis-related genes and WRKY transcription factors, which have been previously implicated in defense response (Shimono et al. 2007) were among the significantly up-regulated fraction (Fig. 7). Analysis of over-representation of functional categories revealed that most number of differentially expressed genes were related to amino acid metabolism followed by starch and lipid biosynthesis (Fig. 8). A significant number of genes were involved in signal transduction pathways, oxidative phosphorylation and secondary metabolite synthesis.

Real-time quantitative PCR for two key defense related genes, WRKY45 and PR1b in NF4050-8 and spl5

An earlier study demonstrated that over-expression of WRKY45 transcription factor gene in rice markedly enhances resistance to rice blast fungus (Shimono et al. 2007). Epistasis analysis revealed that WRKY45 is involved in a signaling pathway downstream of SA but independent of NH1, while PR1a and PR1b are considered good indicators of active NH1 pathway in rice (Shimono et al. 2007). In order to ascertain what pathways are most likely active in the NF4050-8 and spl5 genotypes, we determined the levels of expression of these two key genes, WRKY45 and PR1b through real-time RT-PCR experiments in samples collected from three different stages viz., NL (no lesion stage), ML (mild lesion stage) and SL (severe lesion stage) (Fig. 9). A transgenic line, which is an over-expressor of WRKY45 was used as positive control in the experiment which evidently gave the highest levels of expression. In the NL stage, there was no significant difference in the expression levels of WRKY45 between control/wild group of genotypes (Nipponbare, CO39, and Kasalath) and mutant genotypes (NF4050-8 and spl5). In the ML stage, significant and similar up-regulation of WRKY45 could be detected in the mutant genotypes, NF4050-8 and spl5. In the SL stage, the expression of WRKY45 came down noticeably but was still higher than the control and NL stage expression levels. Similarly, expression levels of PR1b, an indicator of active NH1 dependent pathway, were considerably higher in ML stage of NF4050-8 and spl5. The spl5 mutant displayed very

Table 2 Candidate ORFs identified in the 35 kb delimited interval on the BAC contig AP004379

Candidate ORFs	TIGR/IRGSP gene identity	Genomic location on chr.7	Gene description	No. of Exons	Gene size (kb)	Coding region % GC content	Putative function
G1	LOC_Os07g09910/ Os07g0197300	5,270,787–5,271,719	Stripe rust resistance protein Yr10, putative	1	0.933	63.1	Defense response; 60% similarity with rice NBS–LRR resistance protein (LOC_Os07g09940)
G2	LOC_Os07g09914/ Os07g0197400	5,275,242–5,277,496	Expressed protein	2	2.254	66.5	Not known
G3	LOC_Os07g09920/ Os07g0197500	5,279,463–5,282,008	Disease resistance protein RPM1, with 'NB–ARC' domain and 'disease resistance' signature	2	2.545	47.7	Defense response, apoptosis and ATP binding. NB–ARC domain is associated with cell death in animals (Van der Biezen and Jones 1998)
G4	LOC_Os07g09930	5,284,091–5,284,950	Transposon protein, putative, unclassified/WRKY17 like element (as per Rice-GAAS annotation)	2	0.859	52.5	Not known/putative transcriptional regulator of defense related genes
G5	Predicted by Rice-GAAS	5,285,360–5,285,894	Putative DNA-directed RNA polymerase I subunit RPA1 (DNA-directed RNA polymerase I largest subunit) (RNA polymerase I 194 kDa subunit) (RPA194) (A190)	1	0.534	71.0	Definite function not known
G6	Predicted by Rice-GAAS	5,288,770–5,289,851	Hypothetical protein similar to blight resistant RGA3 like protein	2	1.08	68.4	Defense response, putative
G7	LOC_Os07g09940/ Os07g0197800	5,291,221–5,292,186	NBS–LRR resistance protein, putative	1	0.966	62.5	Defense response

Table 3 Significant ($P < 0.05$) differentially expressed genes with more than threefold expression in the lesion mimic mutant, NF4050-8

Probe name	Description	Up/down	Fold change (WT/mutant)
AK105226	Zn finger, C_2H_2 type domain containing protein	Up	16.6
AF306651	Pathogenesis-related protein 1 precursor	Up	15.2
AK060877	Lectin-like receptor kinase 7;2	Up	13.1
AK066488	Subtilase	Up	12.8
AK061045	Peptidase A1, pepsin family protein	Up	12.3
AK066255	WRKY transcription factor 45	Up	12.3
AK109770	WRKY transcription factor 49	Up	12.3
AK100029	*S*-adenosyl-L-methionine:salicylic acid carboxyl methyltransferase	Up	12.1
Os11g0514400	Brassinosteroid insensitive 1-associated receptor kinase 1 precursor (EC 2.7.1.37)	Up	10.9
AK108406	FYVE/PHD zinc finger domain containing protein	Up	10.8
AK065631	von Willebrand factor, type A domain containing protein	Up	10.8
CI417720	Helix-turn-helix, Fis-type domain containing protein	Up	10.6
AK106264	Mucin-like protein	Up	10.6
AK059767	Chitinase 1 precursor (EC 3.2.1.14) (tulip bulb chitinase-1) (TBC-1)	Up	9.8
AK110695	Flavodoxin/nitric oxide synthase domain containing protein	Up	9.6
AK065988	PDR-like ABC transporter (PDR4 ABC transporter)	Up	9.3
AK121163	Mlo-related protein family protein	Up	9.1
AK068958	Signal recognition particle 54 kDa protein 2 (SRP54)	Up	9.1
CI444008	CDPK substrate protein 1	Up	9.1
AK064115	ARK3 product/receptor-like serine/threonine protein kinase ARK3	Up	9.0
CI422599	GroES-like domain containing protein	Up	8.9
AK099018	EGF-like calcium-binding domain containing protein	Up	8.9
AK061923	Catalase isozyme A (EC 1.11.1.6) (CAT-A)	Up	8.8
AK061433	Heat stress transcription factor Spl7 (heat shock factor RHSF10)	Up	8.6
AK107926	Pathogenesis-related protein 1 precursor (PR-1b)	Up	8.2
AK058637	Alpha-amylase/trypsin inhibitor (antifungal protein)	Up	7.9
AK065939	SNF2-related domain containing protein	Up	7.5
CI362407	Low affinity calcium antiporter CAX2	Up	7.0
AB027421	Class III chitinase homolog (OsChib3H-b)	Up	7.0
AK069860	Chitinase (EC 3.2.1.14).	Up	6.7
AK060261	Abscisic stress ripening protein 1	Up	6.6
AK063834	NADPH HC toxin reductase	Up	6.1
AF200467	Subtilisin-like secreted protease	Up	5.8
AK107989	Pathogenesis-related transcriptional factor and ERF domain containing protein	Up	5.2
AK069603	BED finger domain containing protein	Up	4.6
AK072667	Vacuolar sorting receptor homolog	Up	4.5
Os04g0432100	GRAS transcription factor domain containing protein	Up	4.5
AK073876	GRAB2 protein	Up	4.3
AF403129	S-locus receptor-like kinase RLK10	Up	3.9
AK058432	SCAMP family protein	Up	3.4
AK058343	Low-temperature induced protein lt101.2.	Up	3.4
AK104388	Heme peroxidase, plant/fungal/bacterial family protein	Down	13.9
AK063090	Tumor-related protein (fragment)	Down	13.0
AK062646	Plastocyanin-like domain containing protein	Down	12.6
AK060639	Plant invertase/pectin methylesterase inhibitor domain containing protein	Down	10.7
AK062278	Beta-Ig-H3/fasciclin domain containing protein	Down	10.1
CI025686	Plant disease resistance response protein family protein	Down	9.5
CI333262	Basic helix-loop-helix dimerisation region bHLH domain containing protein	Down	9.1

Table 3 continued

Probe name	Description	Up/down	Fold change (WT/mutant)
Os09g0351700	Protein kinase family protein	Down	9.1
AF261271	Beta-expansin precursor	Down	8.6
AK121173	Rapid ALkalinization Factor family protein	Down	8.4
AK071366	Dehydrin family protein	Down	8.4
AK061430	Harpin-induced 1 domain containing protein	Down	7.7
AK061610	Plant lipoxygenase family protein	Down	7.0
AK068862	Myo-inositol oxygenase	Down	7.0
AK060670	DNA-damage-repair/toleration protein DRT100 precursor	Down	6.8
AF072695	Rhicadhesin receptor precursor (germin-like protein)	Down	6.8
AK066624	Thaumatin, pathogenesis-related family protein	Down	6.7
CI197948	Protein kinase domain containing protein	Down	6.6
AK063881	Universal stress protein (Usp) family protein	Down	6.4
AK065545	BTB/POZ domain containing protein	Down	6.1
CI526382	TGF-beta receptor, type I/II extracellular region family protein	Down	6.0
AK121015	Trehalose-6-phosphate phosphatase	Down	5.9
AK106866	Zn-finger, RING domain containing protein	Down	5.9
Os02g0318500	PDR-like ABC transporter (PDR2 ABC transporter)	Down	5.8
AK062365	Auxin induced protein	Down	5.8
AK059813	I-box binding factor (fragment)	Down	5.7
AK065846	Bowman-Birk trypsin inhibitor	Down	5.6
AK102794	NAC-domain containing protein 21/22 (ANAC021) (ANAC022)	Down	5.4
Os10g0489000	GRAM domain containing protein	Down	5.3
AK070856	NBS–LRR disease resistance protein homolog (fragment)	Down	5.2
AK106769	BABY BOOM	Down	5.1
AK104576	Ethylene response factor 2	Down	5.1
AK060770	Respiratory burst oxidase homolog	Down	5.0
AK066541	Serine/threonine protein kinase	Down	4.9
AK058438	RelA/SpoT domain containing protein	Down	4.9
AK104709	ABC transporter related domain containing protein	Down	4.9
AK108057	Chaperone protein dnaJ (40 kDa heat shock chaperone protein) (HSP40)	Down	4.9
AK060976	NAC-domain containing protein 21/22 (ANAC021) (ANAC022). Splice isoform 2	Down	4.7
AK069499	Wound-induced WI12 family protein	Down	4.6
AK062952	NAM protein	Down	4.6
AK060193	Tonoplast membrane integral protein ZmTIP4-2	Down	4.5
AK070467	Bowman-Birk type proteinase inhibitor (EBI)	Down	4.4
AK065697	Heat shock protein DnaJ, N-terminal domain containing protein	Down	4.4
AK067875	Multi antimicrobial extrusion protein MatE family protein	Down	4.3
CI446243	TRANSPARENT TESTA 12 protein	Down	4.2
AK059636	NADPH-dependent codeinone reductase (EC 1.1.1.247)	Down	4.2
AK061626	Thylakoid membrane phosphoprotein 14 kDa, chloroplast precursor	Down	4.2
AY327041	Receptor-like kinase	Down	4.0
AK071957	Receptor protein kinase	Down	4.0
AK104654	Auxin-responsive protein (Aux/IAA) (fragment)	Down	3.9
AB029508	Small GTP-binding protein OsRac1	Down	3.9
CI444468	DNA-binding WRKY domain containing protein	Down	3.9
Os11g0673900	NBS–LRR type resistance protein (fragment)	Down	3.9
AK064101	Cyclin-like F-box domain containing protein	Down	3.8
AK068104	LIGULELESS1 protein	Down	3.8

Table 3 continued

Probe name	Description	Up/down	Fold change (WT/mutant)
AK101029	Homeobox domain containing protein	Down	3.7
AK111566	Senescence-associated protein 15	Down	3.7
C98212	Basic-leucine zipper (bZIP) transcription factor domain containing protein	Down	3.7
AK106623	E1 protein and Def2/Der2 allergen family protein	Down	3.6
AK063207	Glutathione *S*-transferase GST 31 (EC 2.5.1.18)	Down	3.6
AK108526	Prenylated rab acceptor PRA1 family protein	Down	3.6
Os01g0952100	Nectarin 1 precursor (EC 1.15.1.1) (superoxide dismutase [Mn])	Down	3.6
AK107908	Homeodomain protein JUBEL1	Down	3.5
CI535252	Protein phosphatase 2C ABI2 (EC 3.1.3.16) (PP2C) (abscisic acid-insensitive 2)	Down	3.5
AK119196	CDPK-related protein kinase (EC 2.7.1.-) (PK421)	Down	3.4
AK067939	BEL1-related homeotic protein 14 (fragment)	Down	3.4
AF243384	CRT/DRE binding factor (transcription factor RCBF4)	Down	3.4
AY364310	Rac GTPase activating protein 1	Down	3.4
AK062860	Short-chain dehydrogenase Tic32	Down	3.3

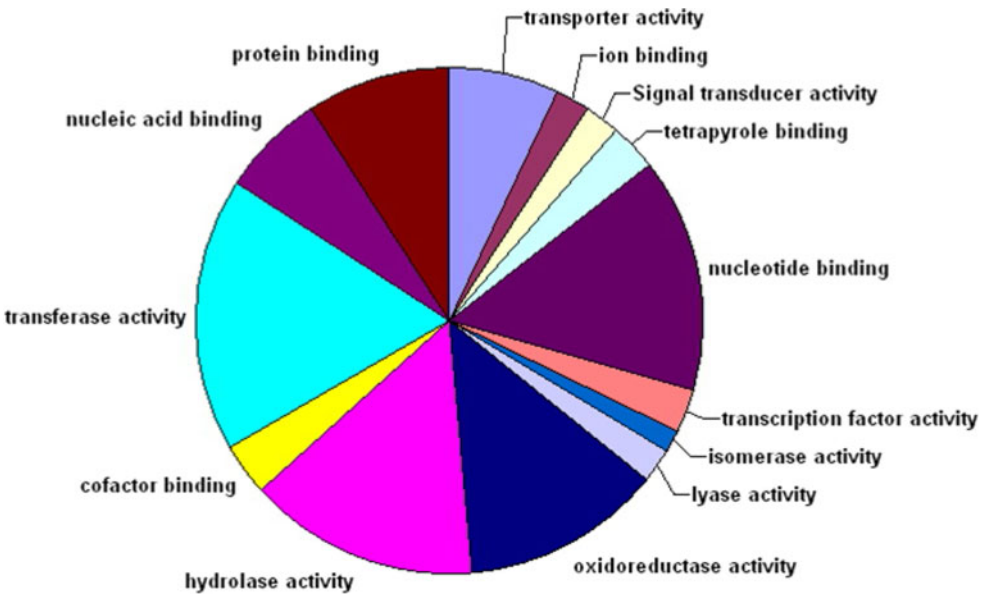

Fig. 7 Microarray analysis of NF4050-8 during progressive lesion appearance stage and grouping of differentially expressed genes according to the putative functions

strong levels of PR1b, almost nine to ten times greater than NF4050-8.

Discussion

Since the initial discovery of lesion mimic mutants in maize, a series of such aberrant genotypes with developmental defects have been identified in Arabidopsis, rice and barley. Interest in such mutants stems from the fact that some of them are associated with enhanced disease resistance, while many others might still be useful in enlightening our knowledge on various molecular mechanisms of programmed cell death (PCD), a phenomenon which has far reaching implications in biology. Unlike lesion mimic mutants in Maize and Arabidopsis, an increased proportion of the spotted leaf mutants in rice is associated with defense response (especially to *M. oryzae* and *X. oryzae*) (Wu et al. 2008) and offer fundamentally different choice of defense genes in practical plant breeding programs that might be more durable in their reaction to pathogen infection. We report here a spotted leaf mutant in rice, NF4050-8 that confers enhanced resistance to at least three different races of *M. oryzae*, isolated from a

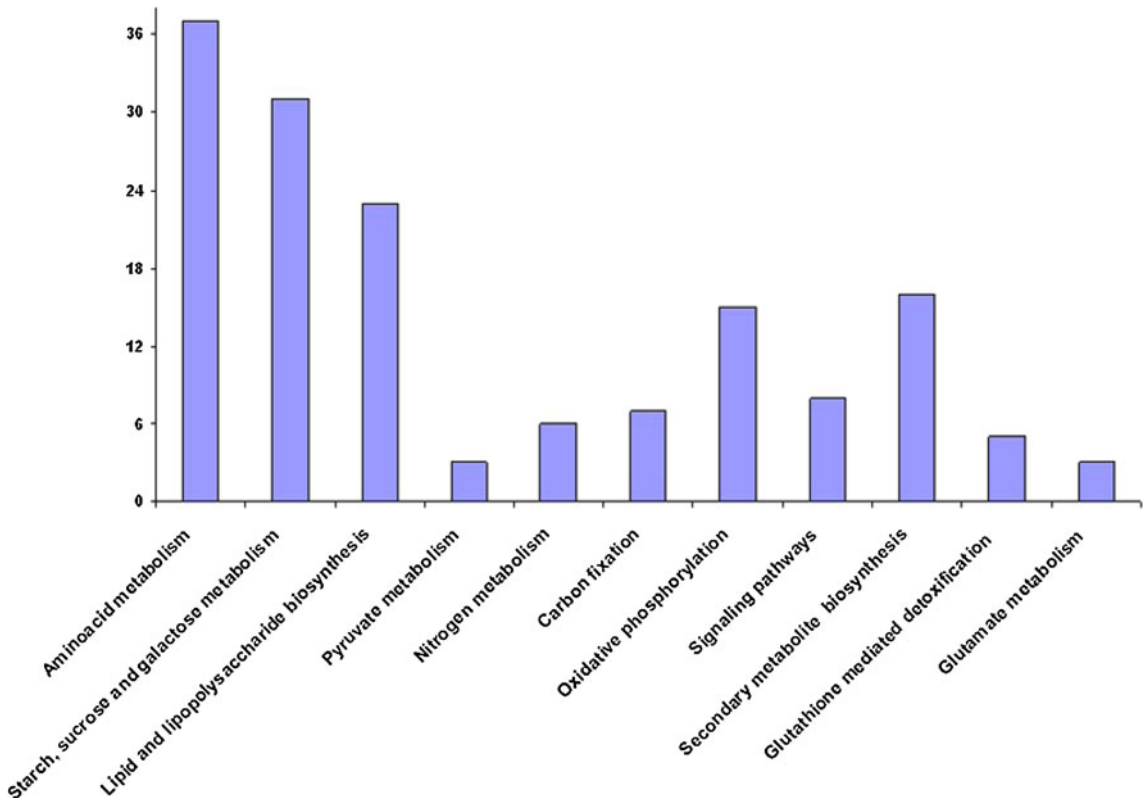

Fig. 8 Analysis of over-representation of functional categories of the differentially expressed genes in NF4050-8 during progressive lesion appearance stage

Tos17 mutant panel available with National Institute of Agrobiological Sciences (NIAS), Tsukuba, Japan. Screening several thousands of lines from this mutant panel for their reaction to different blast races along with a collection of spotted leaf mutant genotypes (designated as *spl* series of mutants) revealed that the isolated NF4050-8 line is similar to spl5 mutant in reaction to three different blast races, lesion appearance and grain yield.

An earlier study based on a japonica × japonica cross had revealed that the lesion mimic phenotype in spl5 is due to single recessive gene located on the short arm of chromosome 7 (Yoshimura et al. 1997). However, inheritance and genetic analysis studies in the present investigation using two segregating F_2 populations of NF4050-8 × CO39 and spl5 × Kasalath revealed that the lesion mimic phenotype in NF4050-8 and spl5 is governed by interaction of at least two genetic factors in indica × japonica crosses, thereby indicating presence of a possible dominant lesion mimic suppression factor in indica genotypes. To our knowledge, this is the first report of an indica factor regulating the expression of single gene governed recessive lesion mimic phenotype in rice. However, it has been well established in maize that the penetrance and expressivity of lesion mimic genes that are inherited in mendelian fashion are significantly influenced by the genetic background in which they reside (Johal 2007). Several inbred lines in maize have been identified which are known to either suppress or exacerbate the symptoms associated with lesion mimic mutants (Neuffer et al. 1983; Gray et al. 1997; Penning et al. 2004; Johal 2007). Extensive genetic studies with *les1* mutant of maize have indicated involvement of multiple genetic factors in development of the phenotype of *les1* (Neuffer et al. 1983; Johal 2007). Besides, genetic factors, environmental factors such as temperature, light intensity and duration, UV composition, etc. have been reported to influence significantly phenotypic expression of lesion mimic mutants in Arabidopsis, maize and rice (Dietrich et al. 1994; Gray et al. 2002; Hoisington et al. 1982; Arase et al. 2000; Fuse et al. 1993; Lorrain et al. 2003).

The lesion mimic mutant line, NF4050-8 identified in this study was isolated from a Tos17 saturation mutant panel created at National Institute of Agrobiological Sciences, Tsukuba, Japan. The endogenous retrotransposon, Tos17 has been shown to be an efficient insertional mutagen in rice for creating saturation mutant lines to study the functions of rice genes (Hirochika 2001). It has been demonstrated that Tos17 is highly active during tissue culture and that the activation of Tos17 is responsible for tissue culture-induced variation (Hirochika 1997). Though

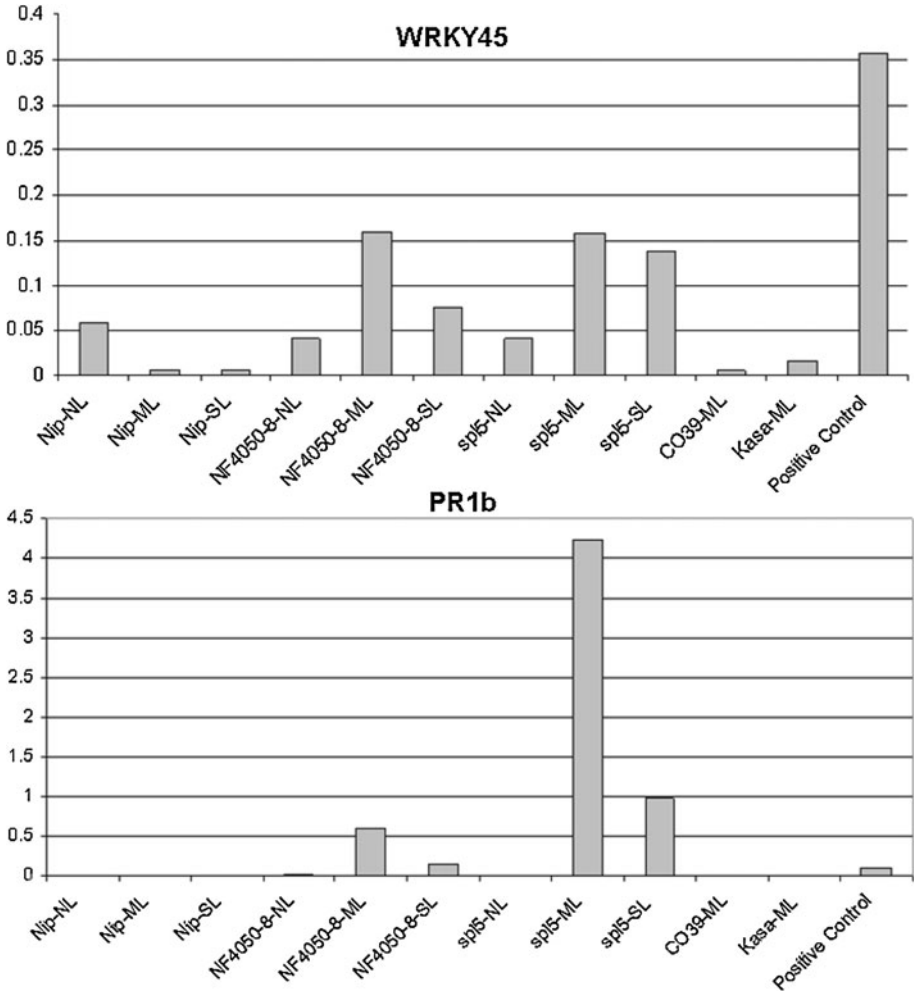

Fig. 9 Quantitative RT-PCR analysis of WRKY45 and PR1b expression during different stages of lesion appearance in spl5 and NF4050-8 mutants. NL (no lesion stage), ML (mild lesion stage) and SL (severe lesion stage)

gene tagging with Tos17 has proven to be a powerful strategy in fishing out the useful genes in rice (Agrawal et al. 2001), one fundamental problem with this reverse genetic resource is relatively low tagging efficiency (5–10%) (Hirochika 2001; Agrawal et al. 2001). Tissue culture-induced mechanisms other than Tos17 insertion such as nucleotide deletion, insertion or base exchanges may cause untagged mutations in high frequency. We report here a novel modified-AFLP procedure, in which three nested Tos17 primers were used in successive PCRs to determine whether a putative mutant line identified by its lesion mimic phenotype from Tos17 mutant panel contains a Tos17 insertion in the target locus. AFLP and southern blot analyses (using Tos17 sequence as probe) of NF4050-8 indicated that the lesion mimic phenotype in this line is most probably due to genetic variation acquired during the tissue culture regeneration process and not due to Tos17 insertion per se. A search for NF4050 mutant line in rice Tos17 sequence database (http://tos.nias.affrc.go.jp/cgi-bin/tos17/ricegenome.cgi) revealed that there are in fact four Tos17 insertions in NF4050 genome out of which two are in chromosome 1 and one each in chromosome 3 and 6. Though this database by no means provides complete information on all possible Tos17 insertion events in any mutant line, it is continuously being updated and the information till date supports the finding of the present investigation that the lesion mimic phenotype of NF4050-8 may not be due to Tos17 insertion per se.

Among the several spl mutants studied till date for their reaction to different races of *M. oryzae,* spl5 had shown consistent and elevated levels of resistance and activation of several defense related genes (Yin et al. 2000; Mizobuchi et al. 2002). In our experience, fine mapping of spl5 is hampered by lack of suitable populations that segregate for lesion mimic symptom in 1:3 ratio. Here, we report fine mapping of a lesion mimic gene from a line identified from Tos17 mutant panel, which resembles spl5 in lesion appearance and plant architecture. The coarse maps constructed with spl5 × Kasalath and NF4050-8 × CO39 populations using SSR markers identified an overlapping region of around 13 cM on short arm of chromosome 7 in rice delimited by RM7479 (31.0 cM) and RM1253 (44.4 cM). RM6574 (38.4 cM) co-segregated with the lesion mimic phenotype in 18 lesion mimic F_2

plants of NF4050-8 × CO39 while RM8247 (41.7 cM) co-segregated with the lesion mimic phenotype in 32 lesion mimic F_2 plants of spl5 × Kasalath. The genetic linkage maps constructed for the lesion mimic locus in this study were consistent with the framework of SSR markers mapped by Panaud et al. (1996), Chen et al. (1997) and Temnykh et al. (2000).

High-resolution mapping using 950 F_3 and 3,821 F_4 plants of NF4050-8 × CO39 that segregate in 1:3 ratio for the lesion mimic symptom identified a candidate region of 35 kb on the BAC accession AP004379. Although SSR markers are relatively abundant in the rice genome, the delimited interval in this study contained only few ready to use SSRs and hence warranted development of several SNP markers for effective delimitation of the candidate region. In several previous studies, SNP markers have proven essential for refining the location of cross-over events around genes of interest in tomato, *Arabidopsis* and rice (Cho et al. 1999; Fridman et al. 2000; Blair et al. 2003). We developed a high throughput SSCP (single strand conformation polymorphism)–SNP assay on our HEGS (high efficiency genome scanning) platform (Kawasaki and Murakami 2000), which is simple, accurate, cost effective and requires neither restriction digestion of the amplification products nor elaborate post-PCR processing detection (Xu et al. 2009). Inside the target region of 1.6 Mb genomic interval flanked by RM21103 and RM21196, 18 SNP markers were developed using HEGS–SSCP system, which led to a marker density of at least one marker per 30–40 kb genomic region. Though a number of SNP assay systems have been reported recently, most of them require either sophisticated instrumentation with large initial investments or suffers from low throughput as compared to many other marker assay systems. The SSCP–SNP assay developed on our HEGS platform is efficient and sensitive to most of the PCR products in the size range of 100–750 bp, requires minimum gel processing time and reasonably high throughput in nature (1,536 SNP data points per person per day) (Xu et al. 2009). Recently, Chen et al. (2009) delimited 80 kb candidate interval for spl5, flanked by SSR7 and RM7121, though this is slightly adjacent to the candidate region identified in the present study for the NF4050-8 causal locus.

The 35 kb genomic interval delimited by the high-resolution mapping contained seven ORFs, five of which are related to defense response and/or cell death and are considered potential candidate genes for the $spl^{NF4050\text{-}8}$ lesion mimic locus. Of the seven ORFs, three coded for hypothetical or expressed proteins with hits to expressed sequence tags (EST) of unknown function, while the rest coded for proteins with hits to ESTs corresponding to genes of known function (Table 2). The three putatively identified defense related genes coding for proteins of known function included stripe rust resistance protein with characteristic LRR domain at the C-terminal portion of the protein, RPM1 like disease resistance protein with NBS–LRR and a cell death associated NB–ARC domain and a disease resistance protein with NBS–LRR domain.

In recent years, a number of gene-for-gene type plant resistance genes (R) have been isolated (Baker et al. 1997; Hammond-Kosack and Jones 1997; Belkhadir et al. 2004), majority of which encode a putative nucleotide binding site (NBS) and a leucine rich repeat (LRR) region and confer resistance to bacteria, viruses, fungi, nematodes, and insects (Baker et al. 1997; Milligan et al. 1998; Rossi et al. 1998; Vos et al. 1998; Belkhadir et al. 2004). It has been demonstrated previously through well conceived experiments that perturbations in NBS–LRR type R genes could indeed lead to cell death and lesion mimicry in maize (Hu et al. 1996; Collins et al. 1999), barley (Büschges et al. 1997; Lyngkjaer et al. 2000) and *Arabidopsis* (Shirano et al. 2002a, b; Noutoshi et al. 2006). Mutations in the complex RP1 locus of maize that controls race specific resistance to the common rust fungus, *Puccinia sorghi* result in lesion mimic phenotype and enhanced resistance (Hu et al. 1996; Collins et al. 1999). Recessive mutations in the barley gene, *Mlo*, induce spontaneous cell death and provide broad-spectrum resistance to all known isolates of the powdery mildew pathogen *Erysiphe graminis* f. sp. *hordei* (Büschges et al. 1997). *Mlo* is thus deduced to be a negative regulator of pathogen resistance and/or cell death. A single amino acid substitution in the NBS region of a semi-dominant locus in *Arabidopsis*, *ssi4*, conferred constitutive expression of several PR (pathogenesis-related) genes, triggered programmed cell death and enhanced resistance to bacterial and oomycete pathogens (Shirano et al. 2002a, b). *SSI4* was found to encode a putative protein belonging to TIR (toll interleukin1 receptor)–NBS–LRR class of R proteins.

The G3 ORF identified in this study contains in addition to a LRR domain at the C-terminal portion, a NB–ARC domain at the N terminus, which is a signaling motif shared by plant resistance gene products and regulators of cell death in animals (Van der Biezen and Jones 1998; van Ooijen et al. 2008). Recent structural molecular modeling of the ARC domain of plant NB–LRR proteins based on the crystal structure of Apaf-1 suggests that this domain is composed of two separate structural units: a N-terminal helical bundle and a C-terminal winged helix domain, referred to as the ARC1 and ARC2 subdomains, respectively (Albrecht and Takken 2006; McHale et al. 2006). With the help of potato Rx protein and domain swap experiments, Rairdan and Moffett (2006), demonstrated that ARC1 subdomain plays a critical role in physically recruiting the LRR to CC–NB–ARC and interplay between ARC2 and LRR domains regulate the molecule's transition

from an inactive to an active state. It has been proposed that NB–LRR proteins are generally present in a cell in a conformation that is auto-inhibited from progressing to an active state due to a perfect fit between LRR and ARC domains but this inactive state is highly sensitive to perturbation such as altered interface between LRR and ARC domains due to an elicitor induced conformational change in LRR (Rairdan and Moffett 2006). It is possible that many autoactivating point mutations in NB–LRR proteins might mimic this process by disrupting negative regulatory regions of the protein. Autoactivating mutations found in human NOD–LRR proteins are numerous and map throughout the proteins in both conserved and non-conserved residues (Tanabe et al. 2004; Ting and Davis 2005; Rairdan and Moffett 2006). While a number of experiments in humans and animals have demonstrated the role of ARC domain and its interaction with LRR in programmed cell death, experimental evidences in plants are scarce. Studying a variety of lesion mimics in plants provide excellent opportunity to uncover such biologically important intramolecular interactions regulating cell death and defense.

The G4 predicted by the Rice-GAAS software analysis in this study corresponds to a transposon like protein with a WRKY17 signature. WRKY proteins play important roles as positive and negative transcriptional regulators of many defense-related genes (Lebel et al. 1998; Li et al. 2004; Robatzek and Somssich 2002). Recently, Noutoshi et al. (2006) identified that a single amino acid insertion in the WRKY domain of the *Arabidopsis* TIR–NBS–LRR–WRKY type disease resistance protein, SLH-1 (sensitive to low humidity 1) caused activation of defense responses and hyper-sensitive cell death. It was demonstrated through gel-shift experiments using a W-box *cis*-element that a 3 bp insertion (leading to single amino acid insertion) in the WRKY domain of SLH1 protein causes a loss of WRKY domain DNA-binding activity. It may be possible that the G4 predicted by Rice-GAAS in this investigation is a C-terminal part of G3, which however would require further experimental verification.

Several previous studies have suggested involvement of at least six classes of genes in plant stress responses (Batista et al. 2008) viz., stress/defense signal perception and transduction, second messengers, ROS-network and SAR response genes, protein modifiers, transcription factors regulating specific stress genes and retrotransposon encoding genes that represent sensitive markers of plant stress. A number of pathogenesis-related defense genes like PR1a/b, chitinases and NADPH HC toxin reductases were significantly up-regulated in the NF4050-8 mutant line suggesting possible activation of more than one defense pathways. In plants, many protein kinases and phosphatases have been reported to be involved in environmental stress responses (Schenk et al. 2000; Xiong and Zhu 2001; Mahalingam et al. 2003) and receptor like kinase in particular is a large superfamily of proteins that is involved in a diverse array of plant responses including development, growth, hormone perception and the response to pathogens. In this study, we found several receptor like kinases; lectin-like receptor kinase (AK060877), brassinosteroid insensitive 1 associated receptor kinase (0s11g0514400), ARK3 product/receptor like serine/threonine protein kinase (AK064115) and S-locus receptor like kinase RLK10 (AF403129) that are significantly up/down-regulated in the mutant line, thus indicating the importance of this group of genes other than that of well known NBS–LRR class of genes to be key players in defense responses. Genes that are involved in the regulation of transcription such as zinc finger of the C_2H_2 type family and genes with WRKY DNA-binding domain were also found to be differentially regulated, which are implicated in stress responses. A significant down-regulation of heme peroxidase gene (AK104388) in NF4050-8 mutant, which otherwise serves as an efficient ROI scavenger may explain severe lesion formation and cell death.

Shimono et al. (2007) earlier demonstrated that WRKY45 plays a crucial and predominant role in BTH (benzothiadiazole) inducible defense responses that strongly enhances resistance to blast infection in rice. The results of their study also established that WRKY45 is neither downstream nor upstream of NH1, a rice homolog of NPR1 and hence appeared to be involved in a pathway independent of NH1, down stream of SA. Significant and similar up-regulation of WRKY45 expression in both NF4050-8 and spl5 mutant genotypes as ascertained by quantitative RT-PCR experiments in this investigation lends credence to the above-mentioned hypothesis that SA signaling pathway mediated by WRKY45 could play an active role in defense responses in rice.

The fine mapping and physical delimitation results presented in this study for NF4050-8 and spl5 mutants will facilitate eventual map based cloning of the causal locus/loci in near future. Conclusions about the spl5 locus relative to other lesion mimic loci in rice is likely to have large-scale implications in extending our knowledge about programmed cell death in plants in general and broad-spectrum resistance against biotic stresses in particular.

References

Agrawal GK, Yamazaki M, Kobayashi M, Hirochika R, Miyao A, Hirochika H (2001) Screening of the rice viviparous mutants generated by endogenous retrotransposon Tos17 insertion. Tagging of a zeaxanthin epoxidase gene and a novel OsTATC gene. Plant Physiol 125:1248–1257

Albrecht M, Takken FLW (2006) Update on the domain architectures of NLRs and R proteins. Biochem Biophys Res Commun 339:459–462

Altschul SF, Madden TL, Schäffer AA, Zhang J, Zhang Z, Miller W, Lipman DJ (1997) Gapped BLAST and PSI-BLAST: a new generation of protein database search programs. Nucleic Acids Res 25:3389–3402

Arase S, Zhao CM, Akimitsu K, Yamamoto M, Ichii M (2000) A recessive lesion mimic mutant of rice with elevated resistance to fungal pathogens. J Gen Plant Pathol 66:109–116

Badigannavar AM, Kale DM, Eapen S, Murty GSS (2002) Inheritance of disease lesion mimic leaf trait in groundnut. J Hered 93:50–52

Baker B, Zambryski P, Staskawicz B, Dinesh-Kumar SP (1997) Signaling in plant–microbe interactions. Science 276:726–733

Batista R, Nelson S, Tiago L, Oliveira MM (2008) Microarray analyses reveal that plant mutagenesis may induce more transcriptomic changes than transgene insertion. Proc Natl Acad Sci USA 105:3640–3645

Belkhadir Y, Subramaniam R, Dangl JL (2004) Plant disease resistance protein signaling: NBS–LRR proteins and their partners. Curr Opin Plant Biol 7:391–399

Blair MW, Hedetale V, Mccouch SR (2002) Fluorescent-labeled microsatellite panels useful for detecting allelic diversity in cultivated rice (*Oryza sativa* L.). Theor Appl Genet 105:449–457

Blair MW, Garris JA, Iyer AS, Chapman B, Kresovich S, Mccouch SR (2003) High resolution genetic mapping and candidate gene identification at the xa5 locus for bacterial blight resistance in rice (*Oryza sativa* L.). Theor Appl Genet 107:62–73

Büschges R, Hollricher K, Panstruga R, Simons G, Wolter M, Frijters A, Daelen RVAN, Van der Lee T, Diergaarde P, Groenendijk J, Topsch S, Vos P, Salamini F, Schulze-Lefert P (1997) The barley *Mlo* gene: a novel control element of plant pathogen resistance. Cell 88:695–705

Chen X, Temnykh S, Xu Y, Cho YG, Mccouch SR (1997) Development of a microsatellite framework map providing genome-wide coverage in rice (*Oryza sativa* L.). Theor Appl Genet 95:553–567

Chen X, Jianwei P, Cheng J, Jiang G, Jin Y, Gu Z, Qian Q, Zhai W, Ma B (2009) Fine genetic mapping and physical delimitation of the lesion mimic gene spotted leaf 5 (spl5) in rice (*Oryza sativa* L.). Mol Breed. doi:10.1007/s11032-009-9299-2

Cho RJ, Mindrinos M, Richards DR, Sapolsky RJ, Anderson M, Drenkard E, Dewdney L, Reuber TL, Stammers M, Federspiel N, Theologis A, Yang WH, Hubbell E, Au M, Chung EY, Lashkari D, Lemieux B, Dean C, Lipshutz RJ, Ausubel FM, Davis RW, Oefner PJ (1999) Genome-wide mapping with biallelic markers in *Arabidopsis thaliana*. Nat Genet 23:203–207

Church GM, Gilbert W (1984) Genomic sequencing. Proc Natl Acad Sci USA 81:1991–1995

Collins N, Drake J, Ayliffe M, Sun Q, Ellis J, Hulbert S, Pryora T (1999) Molecular characterization of the maize *Rp1-D* rust Resistance haplotype and its mutants. Plant Cell 11:1365–1376

Conesa A, Götz S (2008) Blast2GO: a comprehensive suite for functional analysis in plant genomics. Int J Plant Genomics 619832

Dangl JL, Mcdowell JM (2006) Two modes of pathogen recognition by plants. Proc Natl Acad Sci USA 103:8575–8576

Dangl JL, Dietrich RA, Richberg MH (1996) Death don't have no mercy: cell death programs in plant–microbe interactions. Plant Cell 10:1793–1807

Dietrich RA, Delaney TP, Uknes SJ, Ward ER, Ryals JA, Dangl JL (1994) *Arabidopsis* mutants simulating disease resistance response. Cell 77:565–577

Dietrich RA, Richberg MH, Schmidt R, Dean C, Dangl JL (1997) A novel zinc finger protein is encoded by the *Arabidopsis* LSD1 gene and functions as a negative regulator of plant cell death. Cell 88:685–694

Fridman E, Pleban T, Zamir D (2000) A recombination hotspot delimits a wild-species quantitative trait locus for tomato sugar content to 484 bp within an invertase gene. Proc Natl Acad Sci USA 97:4718–4723

Fuse T, Iba K, Satoh H, Nishimura M (1993) Characterization of a rice mutant having an increased susceptibility to light stress at high temperature. Physiol Plant 89:799–804

Gray J, Close PS, Briggs SP, Johal GS (1997) A novel suppressor of cell death in plants encoded by the Lls1 gene of maize. Cell 89:25–31

Gray J, Janick-Buckner D, Buckner B, Close PS, Johal GS (2002) Light-dependent death of maize *lls1* cells is mediated by mature chloroplasts. Plant Physiol 130:1894–1907

Greenberg JT, Ausubel FM (1993) Arabidopsis mutants compromised for the control of cellular damage during pathogenesis and aging. Plant J 4:327–341

Greenberg JT, Guo A, Klessig DF, Ausubel FM (1994) Programmed cell death in plants: a pathogen-triggered response activated coordinately with multiple defense functions. Cell 77:551–563

Hammond-Kosack KE, Jones JDG (1997) Plant disease resistance genes. Ann Rev Plant Physiol Plant Mol Biol 48:575–607

Hayashi N (2005) MAFF microorganism genetic resources manual. In: Rice blast fungus, vol 18. National Institute of Agrobiological Sciences, Tsukuba

Hirochika H (1997) Retrotransposons of rice: their regulation and use for genome analysis. Plant Mol Biol 35:231–240

Hirochika H (2001) Contribution of the *Tos17* retrotransposon to rice functional genomics. Curr Opin Plant Biol 4:118–122

Hirochika H, Sugimoto K, Otsuki Y, Tsugawa H, Kanda M (1996) Retrotransposons of rice involved in mutations induced by tissue culture. Proc Natl Acad Sci USA 93:7783–7788

Hoisington DA, Neuffer MG, Walbot V (1982) Disease lesion mimics in maize. I. Effect of genetic background, temperature, developmental age, and wounding on necrotic spot formation with Les1. Dev Biol 93:381–388

Hu G, Richter TE, Hulbert SH, Pryor T (1996) Disease lesion mimicry caused by mutations in the rust resistance gene *rpl*. Plant Cell 8:1367–1376

Hu G, Yalpani N, Briggs SP, Johal GS (1998) A porphyrin pathway impairment is responsible for the phenotype of a dominant disease lesion mimic mutant of maize. Plant Cell 10:1095–1106

Iwata N, Omura T, Satoh H (1978) Linkage studies in rice (*Oryza sativa* L.). On some mutants for physiological leaf spots. J Fac Agric Kyushu Univ 22:243–251

Johal GS (2007) Disease lesion mimic mutants of maize. APSnet. http://www.apsnet.org/online/feature/mimics/default.asp. Accessed 24 Jan 2008

Johal GS, Hulbert S, Briggs SP (1995) Disease lesion mimics of maize: a model for cell death in plants. Bioessays 17:685–692

Kawasaki S, Murakami Y (2000) Genome analysis of *Lotus japonicus*. J Plant Res 113:497–506

Kottapalli KR, Rakwal R, Satoh K, Shibato J, Kottapalli P, Iwahashi H, Kikuchi S (2007) Transcriptional profiling of indica rice cultivar IET8585 (Ajaya) infected with bacterial leaf blight pathogen *Xanthomonas oryzae* pv. *oryzae*. Plant Physiol Biochem 45:834–850

Larkin PJ, Scowcroft WR (1981) Somaclonal variation: a novel source of variability from cell culture for plant improvement. Theor Appl Genet 60:197–214

Lebel E, Heifetz P, Thorne L, Uknes S, Ryals J, Ward E (1998) Functional analysis of regulatory sequences controlling PR-1 gene expression in Arabidopsis. Plant J 16:223–233

Li J, Brader G, Palva ET (2004) The WRKY70 transcription factor: a node of convergence for jasmonate-mediated and salicylate-mediated signals in plant defense. Plant Cell 16:319–331

Lorrain S, Vailleau F, Balague C, Roby D (2003) Lesion mimic mutants: keys for deciphering cell death and defense pathways in plants? Trends Plant Sci 8:263–271

Lyngkjaer MF, Newton AC, Atzema JL, Baker SJ (2000) The Barley *mlo*-gene: an important powdery mildew resistance source. Agronomie 20:745–756

Mahalingam R, Gomez-Buitrago A, Eckardt N, Shah N, Guevara-Garcia A, Day P, Raina R, Fedoroff NV (2003) Characterizing the stress/defense transcriptome of *Arabidopsis*. Genome Biol 4:R20.1–R20.14

Mchale L, Tan X, Koehl P, Michelmore RW (2006) Plant NBS–LRR proteins: adaptable guards. Genome Biol 7:212

Milligan SB, Bodeau J, Yaghoobi J, Kaloshian I, Zabel P, Williamson VM (1998) The root knot nematode resistance gene *Mi* from tomato is a member of the leucine zipper, nucleotide binding, leucine-rich repeat family of plant genes. Plant Cell 10:1307–1319

Mizobuchi R, Hirabayashi H, Kaji R, Nishizawa Y, Yoshimura A, Satoh H, Ogawa T, Okamoto M (2002) Isolation and characterization of rice lesion-mimic mutants with enhanced resistance to rice blast and bacterial blight. Plant Sci 163:345–353

Mori M, Tomita C, Sugimoto K, Hasegawa M, Hayashi N, Dubouzet JG, Ochiai H, Sekimoto H, Hirochika H, Kikuchi S (2007) Isolation and molecular characterization of a *Spotted leaf 18* mutant by modified activation-tagging in rice. Plant Mol Biol 63:847–860

Nair SK, Tomar SMS (2001) Genetical and anatomical analyses of a leaf flecking mutant in wheat. Euphytica 121:53–58

Neuffer MG, Hoisington DA, Walbot V, Pawar SE (1983) The genetic control of disease symptoms. In: Gene structure and function in higher plants. Oxford/IBH Pub. Co, New Delhi, pp 123–124

Noutoshi Y, Kuromori T, Wada T, Hirayama T, Kamiya A, Imura Y, Yasuda M, Nakashita H, Shirasu K, Shinozaki K (2006) Loss of NECROTIC SPOTTED LESIONS 1 associates with cell death and defense responses in *Arabidopsis thaliana*. Plant Mol Biol 62:29–42

Panaud O, Chen X, Mccouch SR (1996) Development of SSR markers and characterization of simple sequence length polymorphism (SSLP) in rice (*Oryza sativa* L.). Mol Gen Genet 16:597–607

Penning BW, Johal GS, Mcmullen MD (2004) A major suppressor of cell death, slm1, modifies the expression of the maize (*Zea mays* L.) lesion mimic mutation les23. Genome 47:961–969

Pryor AJ (1987) The origin and structure of fungal disease resistance genes in plants. Trends Genet 3:157–161

Rairdan GJ, Moffett P (2006) Distinct domains in the ARC region of the potato resistance protein Rx mediate LRR binding and inhibition of activation. Plant Cell 18:2082–2093

Robatzek S, Somssich IE (2002) Targets of AtWRKY6 regulation during plant senescence and pathogen defense. Genes Dev 16:1139–1149

Rossi M, Goggin FL, Milligan SB, Kaloshian I, Ullman DE, Williamson VM (1998) The nematode resistance gene *Mi* of tomato confers resistance against the potato aphid. Proc Natl Acad Sci USA 95:9750–9754

Schenk PM, Kazan K, Wilson I, Anderson PJ, Richmond T, Somerville SC, Manners JM (2000) Coordinated plant defense responses in *Arabidopsis* revealed by microarray analysis. Proc Natl Acad Sci USA 97:11655–11660

Shah J, Kachroo P, Klessig DF (1999) The *Arabidopsis ssi1* mutation restores pathogenesis-related gene expression in *npr1* plants and renders defensin gene expression salicylic acid dependent. Plant Cell 11:191–206

Sharov AA, Dudekula DB, Ko MS (2005) A web-based tool for principal component and significance analysis of microarray data. Bioinformatics 21:2548–2549

Shimono M, Sugano S, Nakayama A, Jiang CJ, Ono K, Toki S, Takatsuji H (2007) Rice WRKY45 plays a crucial role in benzothiadiazole-inducible blast resistance. Plant Cell 19:2064–2076

Shirano Y, Kachroo P, Shah J, Klessig DF (2002a) A gain-of-function mutation in an Arabidopsis Toll Interleukin1 receptor-nucleotide binding site-leucine-rich repeat type R gene triggers defense responses and results in enhanced disease resistance. Plant Cell 14:3149–3162

Shirano Y, Kachroo P, Shah J, Klessig DF (2002b) A gain-of function mutation in an *Arabidopsis* toll interleukin1 receptor nucleotide binding site-leucine-rich repeat type R gene triggers defense responses and results in enhanced disease resistance. Plant Cell 14:3149–3162

Takahashi A, Kawasaki T, Henmi K, Shi IK, Kodama O, SATOH H, Shimamoto K (1999) Lesion mimic mutants of rice with alterations in early signaling events of defense. Plant J 17:535–5453

Tanabe T, Chamaillard M, Ogura Y, Zhu L, Qiu S, Masumoto J, Ghosh P, Moran A, Predergast MM, Tromp G, Williams CJ, Inohara N, Núñez G (2004) Regulatory regions and critical residues of NOD2 involved in muramyl dipeptide recognition. EMBO J 23:1587–1597

Temnykh S, Park NA, Cartinhour S, Hauck N, Lipovich L, Cho YG, Ishii T, Mccouch SR (2000) Mapping and genome organization of microsatellite sequences in rice (*Oryza sativa* L.). Theor Appl Genet 100:697–712

Ting JP, Davis BK (2005) CATERPILLER: a novel gene family important in immunity, cell death, and diseases. Annu Rev Immunol 23:387–414

van der Biezen EA, Jones JDG (1998) The NB-ARC domain: a novel signaling motif shared by plant resistance gene products and regulators of cell death in animals. Curr Biol 8:R226–R227

van Ooijen G, Mayr G, Kasiem MMA, Albrecht M, Cornelissen BJC, Takken FLW (2008) Structure–function analysis of the NB-ARC domain of plant disease resistance proteins. J Exp Bot 59:1383–1397

Vos P, Hogers R, Bleeker M, Reijans M, van de Lee T, Hornes M, Frijters A, Pot J, Peleman J, Kuiper M (1995) AFLP: a new technique for DNA fingerprinting. Nucleic Acids Res 23:4407–4414

Vos P, Simons G, Jesse T, Wijbrandi J, Heinen L, Hogers R, Frijters A, Groenendijk J, Diergaarde P, Reijans M, Fierens-Onstenk J, de Both M, Peleman J, Liharska T, Hontelez J, Zabeau M (1998) The tomato *Mi-1* gene confers resistance to both root-knot nematodes and potato aphids. Nat Biotechnol 16:1365–1369

Wolter M, Hollricher K, Salaminip F, Schulze-Lefert P (1993) The mlo resistance alleles to powdery mildew infection in barley trigger a developmentally controlled defense mimic phenotype. Mol Gen Genet 239:122–128

Wu J, Mizuno H, Hayashi-Tsugane M, Ito Y, Chiden Y, Fujisawa M, Katagiri S, Saji S, Yoshiki S, Karasawa W, Yoshihara R, Hayashi A, Kobayashi H, Ito K, Hamada M, Okamoto M, Ikeno M, Ichikawa Y, Katayose Y, Yano M, Matsumoto T, Sasaki T (2003) Physical maps and recombination frequency of six rice chromosomes. Plant J 36:720–730

Wu C, Bordeos A, Madamba MRS, Baraoidan M, Ramos M, Wang GL, Leach JE, Leung H (2008) Rice lesion mimic mutants with enhanced resistance to diseases. Mol Genet Genomics 279:605–619

Xiong L, Zhu JK (2001) Abiotic stress signal transduction in plants: molecular and genetic perspectives. Physiol Plant 112:152–166

Xu X, Kawasaki S, Fujimura T, Wang CT (2005) A protocol for high throughput extraction of DNA from rice leaves. Plant Mol Biol Rep 27:291–295

Xu X, Chen H, Fujimura T, Kawasaki S (2008) Fine mapping of a strong QTL of field resistance against rice blast, Pikahei-1(t), from upland rice Kahei, utilizing a novel resistance evaluation system in the greenhouse. Theor Appl Genet 117:997–1008

Xu X, Babu R, Fujimura T, Kawasaki S (2009) A high-throughput, low cost gel-based SNP assay for positional cloning and marker assisted breeding of useful genes in cereals. Plant Breed 128:325–331

Yamanouchi U, Yano M, Lin H, Ashikari M, Yamada K (2002) A rice spotted leaf gene, *Spl7*, encodes a heat stress transcription factor protein. Proc Natl Acad Sci USA 99:7530–7535

Yin Z, Chen J, Zeng L, Goh M, Leung H, Khush GS, Wang GL (2000) Characterizing rice lesion mimic mutants and identifying a mutant with broad-spectrum resistance to rice blast and bacterial blight. Mol Plant Microbe Interact 13:869–876

Yoshimura A, Ideta O, Iwata N (1997) Linkage map of phenotype and RFLP markers in rice. Plant Mol Biol 35:49–60

Yu J, Hu S, Wang J, WONG GK, Li S et al (2002) A draft sequence of the rice genome (*Oryza sativa* L. ssp. indica). Science 296:79–92

Zeng LR, Qu S, Bordeos A, Yang C, Baraoidan M, Yan H, Xie Q, Nahm BH, Leung H, Wang GL (2004) *Spotted leaf11*, a negative regulator of plant cell death and defense, encodes a U-Box/Armadillo repeat protein endowed with E3 ubiquitin ligase activity. Plant Cell 16:2795–2808

Zhang QF, Shen BZ, Dai XK, Mei MH, Maroof MAS, Li ZB (1994) Using bulked extremes and recessive class to map genes for photoperiod-sensitive genic male sterility in rice. Proc Natl Acad Sci USA 91:8675–8679